FRONTIERS OF PHYSICS

TOPICAL REVIEW
Volume 18 / Issue 4 / 43601 / 2023

Review of the role of ionic liquids in two-dimensional materials

Na Sa[1], Meng Wu[1,†], Hui-Qiong Wang[1,2,‡]

1 Engineering Research Center of Micro-nano Optoelectronic Materials and Devices, Ministry of Education; Fujian Key Laboratory of Semiconductor Materials and Applications, CI Center for OSED, and Department of Physics, Xiamen University, Xiamen 361005, China
2 Department of Physics, and Department of New Energy Science and Engineering, Xiamen University Malaysia, Sepang 43900, Malaysia
Corresponding authors. E-mail: †meng.wu@xmu.edu.cn, ‡hqwang@xmu.edu.cn
Received November 10, 2022; accepted January 9, 2023

ABSTRACT

Ionic liquids (ILs) are expected to be used as readily available "designer" solvents, characterized by a number of tunable properties that can be obtained by modulating anion and cation combinations and ion chain lengths. Among them, its high ionicity is outstanding in the preparation and property modulation of two-dimensional (2D) materials. In this review, we mainly focus on the ILs-assisted exfoliation of 2D materials towards large-scale as well as functionalization. Meanwhile, electric-field controlled ILs-gating of 2D material systems have shown novel electronic, magnetic, optical and superconducting properties, attracting a broad range of scientific research activities. Moreover, ILs have also been extensively applied in various field practically. We summarize the recent developments of ILs modified 2D material systems from the electrochemical, solar cells and photocatalysis aspects, discuss their advantages and possibilities as "designer solvent". It is believed that the design of ILs accompanying with diverse 2D materials will not only solve several scientific problems but also enrich materials design and engineer of 2D materials.

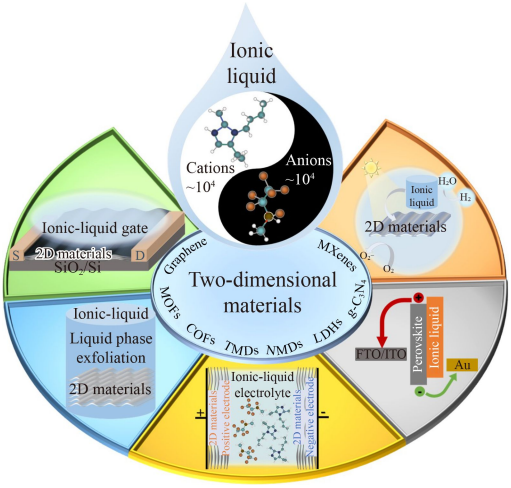

Keywords ionic liquids, two-dimensional materials, liquid phase exfoliation, ionic liquid-gating, electrochemical capacitors, solar cells, photocatalysis

Contents

1 Introduction

Environmental issues are currently one of the major

https://doi.org/10.1007/s11467-023-1258-6

issues world-widely, and the extensive use of destructive solvents and their non-degradable volatility inevitably add to environmental burden [1–3]. As a potential alternative solvent, researches on ILs have gradually proliferated since the first review on "*Room-temperature ionic liquids: synthetic and catalytic solvents*" was published in *Chemical Reviews* in 1999 by Welton [1]. Accompanying with the extensive researches of ILs in chemical synthesis and catalysis, notable reviews of ILs with applications in biomedicine [4, 5], energy materials and storage [6–10] and electrochemical [11] fields have been reported. In this article, we will summarize the recent development of ILs with a different perspective.

It is well known that ILs are salts composed of inorganic anions and organic cations with melting points below 100 °C [12]. IL solvents can be easily designed with desired physicochemical properties and functionalities by varying different combinations of cations and anions assigned to them [13–17]. ILs as solvents generally have the following features: i) they are good solvents for a wide range of inorganic and organic materials, which can bring different combinations of reagents into the same phase and become a substitute for various volatile organic solvents, inorganic acids, alkalis, solid acids, etc.; ii) they are usually composed of poorly coordinated ions, resulting in highly polarity; iii) they are incompatible with many organic solvents, providing non-aqueous polar alternatives for two-phase systems where hydrophobic ILs can be used as water-immiscible polar phases; iv) ILs are non-volatile due to the electrostatic interactions between ions, which can be used to eliminate the sealing problems, enabling the applications in high vacuum systems. Due to the high ionic concentration and the strong interaction between ions, ILs show novel applications in various fields, particularly in two-dimensional (2D) material systems which will be expanded later.

Since graphene, i.e., a single atomic layer of graphite material, was successfully isolated by Geim's group at the University of Manchester in 2004 [18, 19], the family of 2D materials has been spreading rapidly [20]. Common 2D materials include: transition metal dichalcogenide (TMDs [21–31] including MoS_2, $MoSe_2$, $MoTe_2$, WS_2, WSe_2, ReS_2, TaS_2, etc.), noble metal dichalcogenides (NMDs: $PdSe_2$, $PtSe_2$, PtS_2, etc.), graphene [32–34], hexanol boron nitride (h-BN) [35, 36], black phosphorus (BP) [37], silicene [38], germanene [39], borophene [40], layered double hydroxide (LDHs), graphite carbon nitrides (g-C_3N_4) [41], MXenes (usually transition metal nitrides or carbides) [42], metal–organic frameworks (MOFs), covalent–organic frameworks (COFs), organic–inorganic hybrid perovskites, transition metal halides, etc. [43]. 2D materials with no dangling bonds, van der Waals (vdW) heterostructures, lateral dimensions of hundreds of nanometers to tens of micrometers and thickness of several atomic layers, exhibit novel physical properties and offer promising applications in electronic, optoelectronic, and energy harvesting devices [44–46]. Large-area, high-quality 2D materials underpin the development of next-generation electronic and optical devices, providing enhanced interfaces to optics and heterostructure devices [47]. The introduction of ILs in 2D materials brings additional tuning approach both for material syntheses and manipulations of novel physical properties [48]. In this paper we focus on some recent developments of ILs in 2D material systems, which will consist of five sections as shown below: i) ILs-assisted exfoliation of 2D materials; ii) ILs-gating modulated physical properties of 2D materials; iii) ILs modified 2D material electrodes towards high electrochemical performance; iv) ILs as organic spacers for chalcogenide crystallization in solar cells; v) ILs as embedding agents in photocatalysis.

2 Basic properties of ionic liquids

As above-mentioned, ILs can exhibit superacidity, basicity, hydrophilicity, water miscibility and water insolubility, depending mainly on the interaction, size, geometry and charge distribution between the different organic cations and inorganic anions [49]. The most widely used cations include ammonium, sulfonium, phosphonium, imidazolium, pyridinium, picolinium, pyrrolidinium, thiazolium, oxazolium and pyrazolium. In particular for room temperature ILs, researches mainly focus on ILs composed of asymmetric N,N-dialkylimidazolium cations (such as 1-butyl-3-methylimidazolium [BMIM] and 1-ethyl-3-methylimidazolium [EMIM]) associated with a variety of anions [1]. Fluorous, chloride, nitrate, acetate, hexafluorophosphate [PF_6] and tetrafluoroborate [BF_4] are commonly used anions [50]. Among them, the most widely investigated ILs are the ones with $[PF_6]^-$ and $[BF_4]^-$ anions, as shown in Fig. 1. In similar ILs, although the cations are the same, small changes in anion type can significantly affect the physicochemical properties. For example, IL with [BMIM] cation and $[PF_6]^-$ anion is immiscible with water, whereas IL with

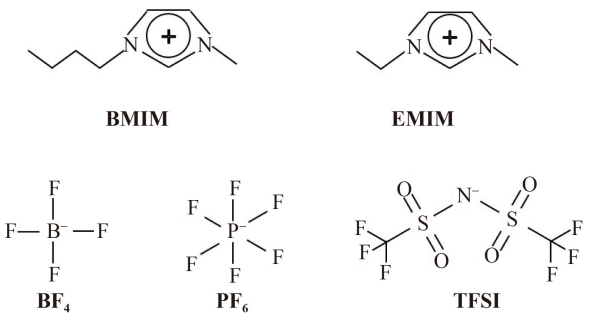

Fig. 1 Frequently used cations and anions in IL. ILs usually consist of N,N-dialkylimidazolium cations (such as 1-butyl-3-methylimidazolium [BMIM] and 1-ethyl-3-methylimidazolium [EMIM]), and anions (hexafluorophosphate [PF_6], tetrafluoroborate [BF_4] and bis (trifluoromethylsulfonyl) imide ([TFSI] or [NTf_2])).

same cation but $[BF_4]^-$ anion is water soluble. The feature that different ion pairs determine the physical and chemical properties of the liquid makes ILs with "designer solvent" property, suggesting that by changing the anions (or cations) the hydrophobicity, viscosity, density and solvation of the IL system may be designed [51].

3 ILs-assisted exfoliation of 2D materials

Controllable fabrication of 2D materials has been of essence for maximizing their low dimensional properties and future practical applications [52–57]. Commonly used methods for preparing single or several layers of nanosheets include chemical vapor deposition, micromechanical cracking, chemical and liquid phase exfoliation (LPE) [58–60]. Among them, LPE was first proposed by Coleman *et al.* [61–63] in 2008 when graphite powder was sonicated by N-methylpyrrolidone (NMP). LPE has become an important technological tool for producing defect-free nanosheets. Proper solvent selection in LPE is the prior consideration that there should be steric repulsion between exfoliated nanosheets and no in-plane adhesion [63, 64]. ILs-assisted exfoliation as a type of LPE exhibits some advantages over organic solvent, such as extremely low vapor pressures, good thermal stability and nonflammability. Due to the strong cation-mediated interactions between ILs and the layered materials, ILs exhibit great advantage in directly exfoliating 2D materials by ultrasonic or microwave irradiation methods to generate highly concentrated nanosheets dispersions [65–68]. In terms of ILs as dispersants for LPE to prepare 2D materials, distinct progress has been made in graphene [69–72]. In these studies, electrostatic interactions between charged ionic species and graphite planar π-electrons were considered to be responsible for the successful exfoliation and stabilization of graphene [73–77]. In fact, exfoliating 2D materials in ILs is similar to the common way of stripping in solution. Dai *et al.* [76] demonstrated that natural graphite flakes (Aldrich, 20 mg) were dispersed in 10 mL of 1-butyl-3-methyl-imidazolium bis(trifluoro-methane-sulfonyl)imide ([BMIM][NTf_2]) and the mixture was subjected to tip sonication using 5–10 min cycles (SONICS, 750 W, 80% amplitude) for a total of 60 min. The resulting dispersion was centrifuged at 10000 rpm for 20 min and the supernatant containing the graphene flakes in IL was collected and retained for use. The precipitate obtained by centrifugation was vacuum filtered through a pre-weighed filter, then washed and dried with ethanol to quantify the amount of unexfoliated or thick graphite flakes. Given the mass of natural graphite flakes used (20 mg), the concentration of suspended graphene in the IL was calculated to be 0.95 $mg \cdot mL^{-1}$. Scanning transmission electron microscopy analysis showed that the dispersion contained flakes with micron-sized edges and only <5 layers. The material was also characterized by X-ray photoelectron spectroscopy and Raman spectroscopy. The surface morphologies of a monolayer and a bilayer graphene with micrometer size using directly [BMIM][NTf_2] IL-assisted exfoliation approach are shown in Figs. 2(a, b). Synthesizing high-quality layered 2D TMD material has been a longstanding challenge. LPE using traditional solvents is improving but suffers from low yields and a long sonication time. However, planar intact laminated MoS_2 sheets had been obtained by LPE of bulk MoS_2 powder using 1-dodecyl-2-pyrrolidone IL through a simple one-pot exfoliation approach by quick sonication [78]. Mandal *et al.* [79] used two cationic polymeric ILs, namely poly(triphenyl-4-vinylbenzylphosphonium chloride) and poly(3-N-butyl-1-vinylimidazolium bromide) to promote the LPE of 2D MoS_2 and $MoSe_2$ in an aqueous medium and found that the obtained MoS_2 suspension showed a thermo-responsive feature, as shown in Fig. 2(c). This method can be extended for efficient generation of $MoSe_2$ nanosheets using the same ILs. In these systems, the polymeric ILs only allow the aqueous exfoliation of metal chalcogenides, and their thermo-responsive property can be attributed to the presence of Cl^- or Br^-. Choosing appropriate functional polymer has been suggested to functionalize TMD nanosheet based on density functional calculations [80, 81].

Wu *et al.* [82] selected a thermo-responsive copolymer of (poly(*N*-isopropylacrylamide-co-IL), PNIL as the model polymer to prepare $MoSe_2$-related nanocomposites, realizing simultaneous exfoliation and noncovalent functionalization of $MoSe_2$ nanosheets. In this system, imidazole rings in PNIL have effective interactions with the layered $MoSe_2$, facilitating the exfoliation to form the PNIL-functionalized $MoSe_2$ nanosheets, for a temperature and photo-dual-responsive nanocomposite hydrogel. However, the temperature-sensitive function of this hydrogel is mainly supported by the poly (N-isopropylacrylamide) moiety rather than the polymeric IL moiety. Inspired by the above works [79–82], Wu *et al.* [83] further used a thermo-responsive polymeric IL (TRPIL) as a universal polymer surfactant to assist the high-efficiency exfoliation of MoS_2, graphite, and h-BN in an aqueous medium through consecutive sonication, as shown in Fig. 2(d). In this case, the reliable interaction between 2D materials and the TRPIL would facilitate the exfoliation and simultaneously achieve a noncovalent functionalization of the exfoliated nanosheets. Interestingly, the dispersion stability of exfoliated nanosheet suspensions can be reversibly tuned by temperature because of the thermo-responsive phase transition behavior of the TRPIL. As a proof of potential applications, a temperature and photo-dual-responsive TRPIL/MoS_2 coloring hydrogel with robust mechanical property and an artificial nacre-like BN nanosheet film with high thermal conductivity were fabricated.

ILs-assisted exfoliation of 2D layered materials is a relatively mature route, and increasing the cationic alkyl chain of ILs to more than 12 carbons converts them into

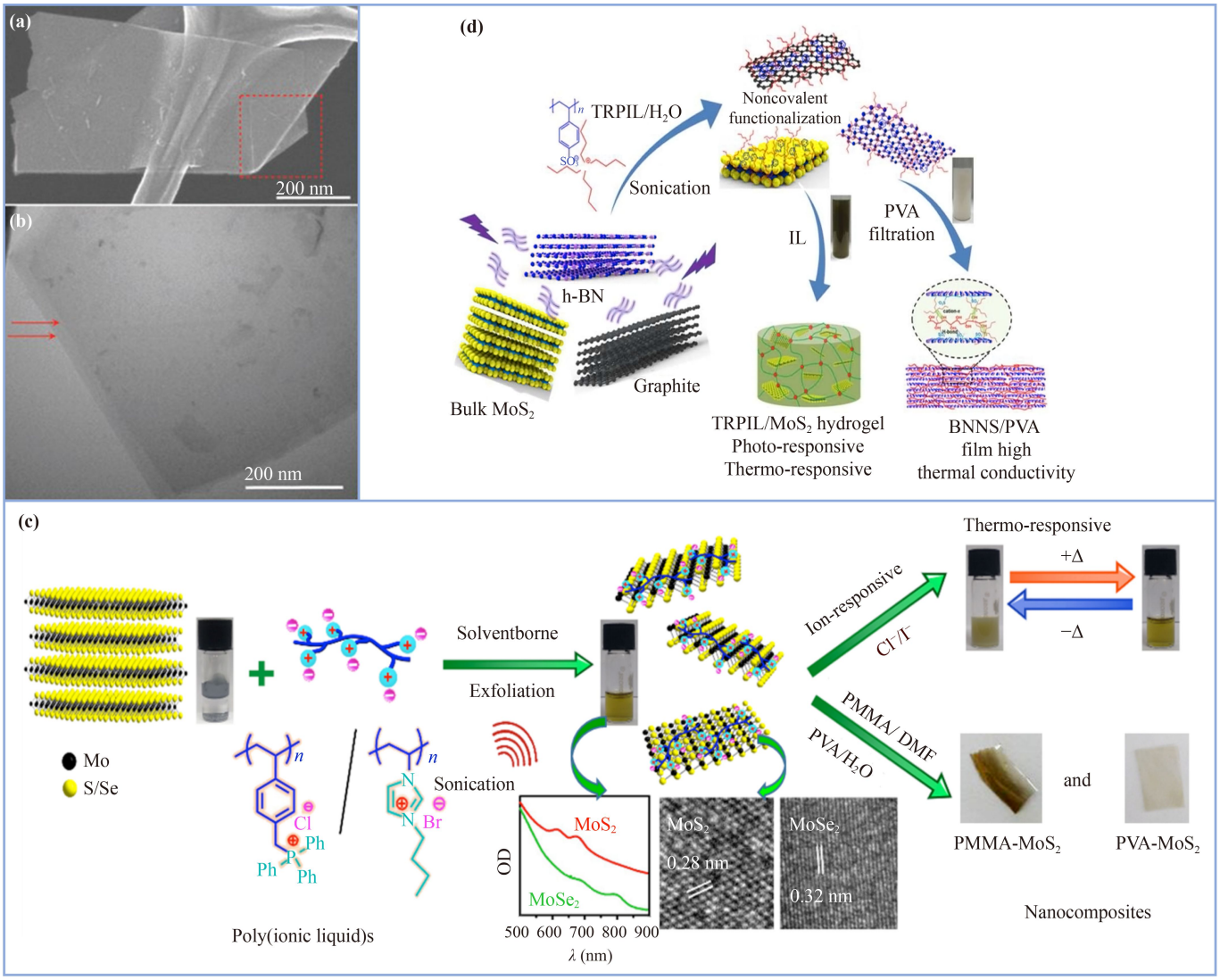

Fig. 2 Direct exfoliation of natural graphite into graphene sheets with micrometer size used [BMIM]-[Tf_2N] IL. Panel **(a)** and **(b)** correspond to a monolayer graphene with folded edges and a bilayer graphene, respectively, Reprinted with permission from Ref. [76], Copyright © 2010 Chemical Communications. **(c)** Schematic view of (P[VBTP][Cl]) and (P[VimBu][Br]) PIL promoted solvent-borne efficient exfoliation of MoS_2/$MoSe_2$ nanosheets for dual-responsive dispersion and polymer nanocomposites. Owing to the solubility in both water and organic solvents, cationic PIL molecules serve the dual purposes of an exfoliating-cum-stabilizing agent. PIL-stabilized nanosheets' dispersions are stable for more than two months at ambient temperature. Reprinted with permission from Ref. [79], Copyright © 2017 ACS. **(d)** Thermally responsive polymeric ILs (TRPIL) act as surfactants to aid the efficient exfoliation and the non-covalent functionalization of exfoliating of MoS_2, graphite, and h-BN. Due to the thermally responsive phase transition behavior of TRPIIL, the dispersion stability of the exfoliated nanosheet suspensions can be reversibly tuned by temperature. Reprinted with permission from Ref. [83], Copyright © 2018 ACS.

smectic IL crystals(ILCs) [84]. Song *et al.* [84] proposed the 1-hexadecyl-3-methylimidazolium chloride ILCs-assisted hydrothermal exfoliation of fluorinated grapheme (FG). The proposed method was efficient for exfoliating FG from bulk fluorinated graphite (FGi) at yield reaching 48%. The well-dispersed homogeneous FG/-poly (vinyl alcohol) (PVA) composite film were fabricated with robust mechanical properties and photothermal effects. Meanwhile, the reliable interaction between FG and ILC led to noncovalent functionalization of exfoliated nanosheets, which were highly stable at room temperature for more than three months without formation of agglomerates. Then, the tribological properties of the exfoliated FG nanosheets were tested as a lubricating additive, and the friction coefficient was significantly reduced by 82% compared with pure water. This also confirms that aromatic cations in IL can interact with graphene through π–π and cation–π interactions [85, 86], thereby improving the problem of low interfacial adhesion of nanomaterials on friction surfaces [87].

Similarly, MoS_2 nanosheets were confined by the ILCs through π–π and C–H···π interactions, preventing direct contact of MoS_2 with water. The ILC–MoS_2 dispersion exhibited remarkable dispersion stability exceeding 8 months at room temperature [88].

In addition to using IL as solvent for LPE, IL-assisted grinding is also a common method to exfoliate 2D materials. The exfoliation of graphene nanosheets and nanodots based on IL-assisted grinding was firstly reported by Shang and co-workers [89]. Wang *et al.* [90] reported one-step synthesis and surface functionalization of MoS_2 nanosheets by a facile IL-assisted grinding method in the presence of chitosan. The selected IL with suitable surface energy could efficiently overcome the van der Waals force between the MoS_2 layers. At present, IL-assisted grinding still needs to be further developed.

4 IL-gating modulated 2D materials

The high carrier density and ionic mobility of ILs have proven to be an efficient manner to drive electronic phase transitions in 2D materials. Electrical double-layer transistors (EDLTs) based on electrostatic ionic gating [91, 92] have been shown to be a versatile tool for achieving novel device functions [93, 94] and inducing new electronic states [95–98] at the interface between ionic media and semiconductor channels. Using IL as the gating layer, the charge carrier density can be up to 10^{15} cm^{-2} at few volts, which has been used to induce many interesting physical properties including insulator-metal transition, unconventional superconductivity, considerable spin–orbit coupling, competition between different quantum phases, etc. [99–103]. Liu *et al.* [104] improved the turn-off characteristics of carbon nanotubes(CNT)-array field-effect transistors (FETs) using an ultra-efficient IL-gating. In particular, it reduces the subthreshold swing (SS) of a typical CNT array FET to 75 mV/decade [Fig. 3(a)]. The SS values of the 30 IL-gated devices were spread over a narrow range with an averaged value of about 90 mV/decade, and some devices even had SS values close to the theoretical limit of 60 mV/decade at room temperature. A direct comparison of an IL-gated CNT array FET (L_{ch} = 290 nm) with an FET with a similar gate length (0.25-μm node with a physical gate length of 0.18 μm) shows that compared to Si PMOS (p-type metal-oxide semiconductor) FETs, CNT array FETs exhibit better on-state current and similar off-state current in a smaller gate source voltage range.

Lezama *et al.* [105] studied $MoTe_2$ with thicknesses over 4 nm, using IL-gated transistors, and demonstrated that bipolar transport on the material surface can be reproduced with hole and electron mobility values between 10 and 30 $cm^2 \cdot V^{-1} \cdot s^{-1}$ at room temperature, as shown in Fig. 3(b). From the surface transport using IL-gated transistors, scanning tunneling spectroscopy and optical transmission spectroscopy analyses, thin $MoTe_2$ layers may exhibit an indirect (E_g = 0.88 eV) to a direct bandgap (E_g = 1.02 eV) transition before mono-layer thickness. Wang *et al.* [106] demonstrated IL-gating of suspended few-layer MoS_2 transistors, where ions can accumulate on both exposed surfaces of free-standing samples. Furthermore, all suspended devices with free-standing MoS_2 layers consistently displayed dramatically improved conductivity and mobility than substrate-supported devices, which suggested the reduction of the Schottky barrier at the metal-semiconductor interfaces and the dielectric screening by ILs. Electrical transport data revealed Schottky emission as the dominated transport mechanism. By modulating IL gating voltage, the suspended MoS_2 devices displayed metal–insulator transition. These results demonstrate that more efficient charge induction can be achieved in suspended 2D materials, which with further optimization, may enable extremely high charge density and novel phase transition, such as the transformation to superconductivity phase as shown below.

Superconductivity is the least studied property in TMDs due to methodological difficulty in accessing it in different TMD species. Wu *et al.* [107] reported the systematic studies of superconductivity in $MoSe_2$, $MoTe_2$ and WS_2 by ionic gating but with different physical mechanisms. IL gating was able to induce superconductivity in $MoSe_2$ based on the dominant electrostatic mechanism, but not in $MoTe_2$ because of inefficient electron accumulation limited by electronic band alignment, as shown in Fig. 3(c). Alternative gating using $KClO_4$/polyethylene glycol enabled a crossover from surface doping to bulk doping, which induced superconductivities in $MoTe_2$ and WS_2 electrochemically. These new varieties greatly enriched the TMD superconductor families and unveiled critical methodology to expand the capability of ionic gating to other materials. However, in 2D TMD systems, some experiments also revealed a marked tendency to a negative electronic compressibility, i.e., the decrease of carrier density with increasing the gate bias, which corresponded to a negative quantum capacitance of the electrons in the TMD transistor [108]. The carrier transport mechanism in these IL-induced low-temperature metallic state is under debates which seems to avoid the superconducting or insulating fate of standard 2D electron systems. Grilli's group [109] suggested an intrinsic nanoscale inhomogeneity to understand the peculiar behavior of the metal-superconductor transition in these IL-gated 2D superconductors. Modeling the system with superconducting puddles embedded in a metallic matrix, they can fit the abnormal temperature-dependent resistivity curves of systems like $TiSe_2$, MoS_2, and ZrNCl. In this framework, the low-temperature debated metallic state can be attributed to the pristine metallic background embedding nonpercolating superconducting clusters. They propose this mechanism based on the interplay between electrons and the charges of the IL-gating, which deepened the understanding of IL-gating systems.

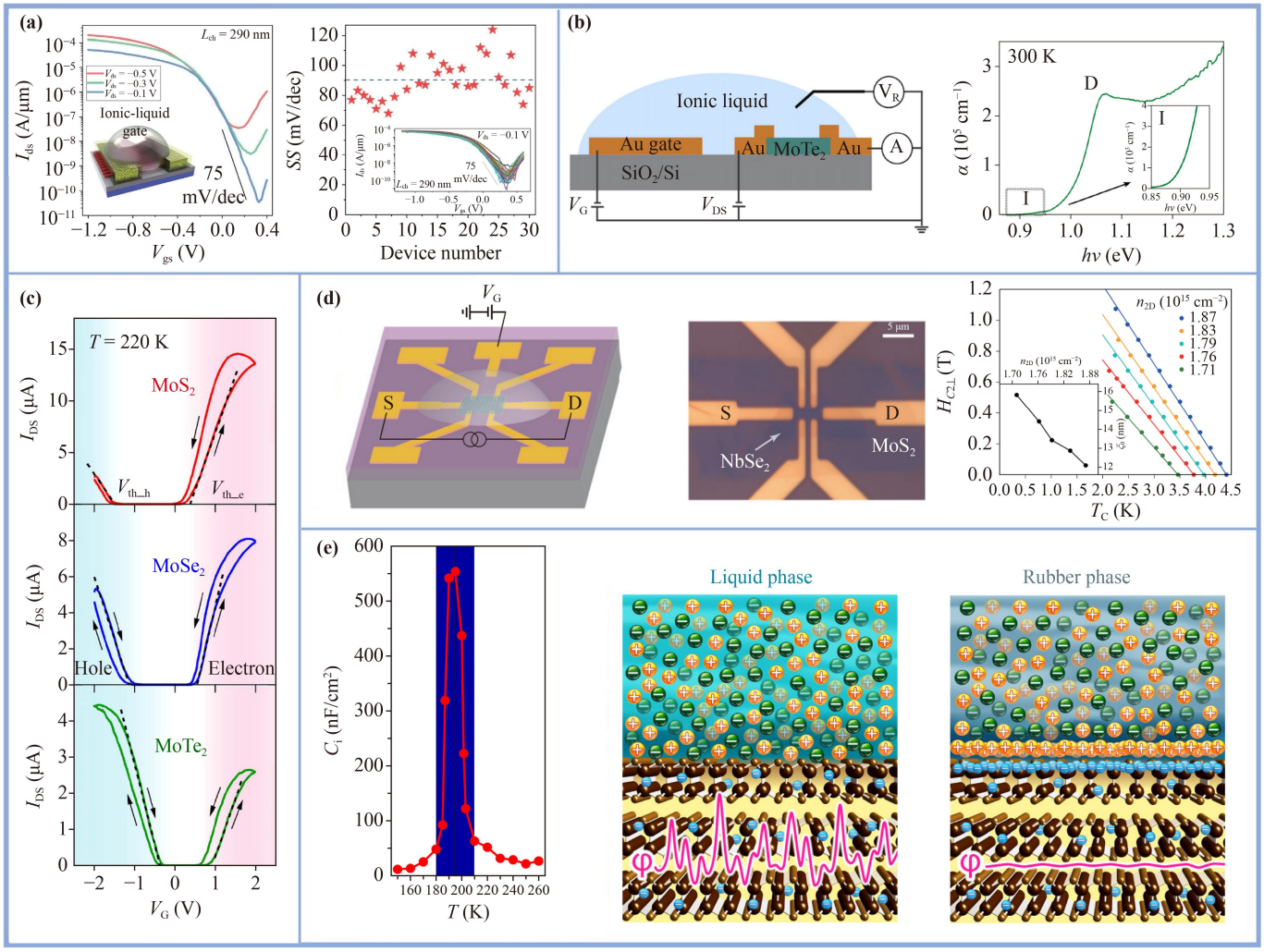

Fig. 3 **(a)** Top-gate FETs fabricated on CNT arrays use IL-gating to maintain low room temperature subthreshold fluctuations of <90 mV per decade. Left is the transfer characteristics of a typical FET with L_{ch} = 290 nm. Right shows the statistic SS distribution of 30 IL-gated devices. Reprinted with permission from Ref. [104], Copyright © 2020 Science. **(b)** Schematic view of an ionic-liquid gated $MoTe_2$ FET with reversible bipolar transmission (left). I and D mark the features corresponding to absorption due to indirect and direct optical transitions (right). Reprinted with permission from Ref. [105], Copyright © 2014 2D Materials. **(c)** Comparisons of typical ambipolar transfer curves of MoS_2, $MoSe_2$ and $MoTe_2$ EDLTs measured with V_{DS} = 0.1 V at 220 K, which exhibit novel superconductivity phase by ionic gating. Reprinted with permission from Ref. [107], Copyright © 2015 Scientific Reports. **(d)** Temperature dependence of the longitudinal sheet resistance and the sheet Hall coefficient at selected gate voltages. IL-gating allows the reversible regulations between superconductivity and CDW order in $NbSe_2$ with variations of the superconducting transition temperature up to ~50 %. Reprinted with permission from Ref. [113], Copyright © 2016 Physical Review Letters. **(e)** T-dependence of the specific capacitance C_i. The IL-f InSe FET manifests an appreciable C_i peak that reaches 550 nF/cm^2 at T = 195 K (left) and schematics illustrating of the intersystem Coulomb interaction-induced self-gating and electrostatic potential profile in the liquid (middle) and rubber phases (right), respectively. φ illustrates the spatial profile of electrostatic potential in InSe. Reprinted with permission from Ref. [115], Copyright © 2022 Nano Letters.

Moreover, the atomically thin TMD metals have unveiled a range of interesting phenomena including the coexistence of charge-density-wave (CDW) ordering and superconductivity down to the monolayer limit [110–112]. Xi *et al.* [113] demonstrate reversible tuning of superconductivity and CDW ordering in model 2D TMD metal $NbSe_2$ by an IL gating approach. A variation up to ~50% in the superconducting transition temperature has been observed, as shown in Fig. 3(d). Both superconductivity and CDW ordering can be strengthened (weakened) by increasing (reducing) the carrier density in 2D $NbSe_2$. The doping dependence of these phase transitions can be understood as driven by a varying electron-phonon coupling strength induced by the gate-modulated carrier density and the electronic density of states near the Fermi surface.

During IL-gating operation, both electrostatic and electrochemical mechanisms may operate for a particular material system. The IL gating-induced metallization may be inhibited in presence of oxygen such as in oxide materials, indicating the favorable of an electrochemical effect therein. However, in more general scenarios, the role of oxygen in the IL-gating is still unclear. Chen *et al.* [114] performed IL-gating experiments on a non-oxide 2D ferromagnetic $Cr_2Ge_2Te_6$. Their results demonstrated that despite the large increase of the gate leakage current in the presence of oxygen, the oxygen did not affect the IL gating effect on the channel resistance of $Cr_2Ge_2Te_6$ devices (<5% difference), suggesting the dominated electrostatic mechanism on non-oxide materials.

Last but not least, ILs alone may undergo temperature-dependent phase transitions, the impact of IL's phase transition on 2D materials is definitely interesting and only has been addressed recently. Cheng *et al.* [115] investigated inter-system Coulomb interactions in IL-functionalized InSe FETs by displacement current measurements at different temperatures, corresponding to the different liquid, rubber and glass phases of the DEME-TFSI ILs, as shown in Fig. 3(e). They found a strong self-gating effect that could increase the interfacial capacitance by a factor of 50, reaching 550 nF/cm^2 in the maximum value at 195 K for the rubber phase of ILs. The detailed IL phase-dependent transport properties, including channel current, carrier mobility, and density, confirms the dominant self-gating at the InSe/IL interface, which paves the way to develop liquid/2D material hybrid devices.

5 IL modified 2D material electrodes

The demand for flexible, powerful and reliable energy distribution and storage is increasingly important with energy challenges [116]. Among the many approaches to energy storage, Electrochemical capacitors (ECs) have some distinct advantages, such as higher power density caused by fast charge/discharge rates (in seconds) and long cycle life (4100 000 cycles) [117], but must further increase its energy density [118]. ECs are mainly composed of electrodes, electrolytes and separators, where researchers attempt to improve the performance of ECs from these three parts. From the calculation formula of the energy density of the capacitor: $E = 1/2\ CV^2$, it can be known that increasing the voltage window of the capacitor can improve the energy density more effectively [119]. Since the voltage V is mainly limited by the stability of the electrolyte, electrolytes retain the focus of research [120–122]. ILs can improve the performance of electrochemical capacitors in two main ways: extended voltage window and efficient utilization of the electrode surface. ILs have received a lot of attention as electrolytes due to their very low vapor pressure, high chemical, thermal and electrochemical stability, and good electrical conductivity especially above room temperature [121, 123–131]. Unlike organic electrolytes, ILs have cell voltages >3 V and can provide longer cycle life even at high voltages above room temperature, advantages that depend on the chemical properties of IL ions [118, 123, 132–135]. It has been shown that the double layer capacitance of carbon electrodes in ILs depends strongly on the ion polarization rate. Applying different biased electric field, the ions exhibit different preferred orientations, which affects the dielectric constant in the double layer capacitor as well as the double layer thickness [123, 136]. Therefore, given the different properties of the positive and negative IL counter ions involved in the double-layer capacitor, the surface characteristics of the positive and negative electrodes will be different, thus giving rise to different supercapacitor configurations. The low melting point, hydrophobicity and high purity of IL create conditions for the long cycle life of high-voltage supercapacitor. In addition to the above advantages, the high ion concentration of ILs and the strong interaction between ions can be adapted by adjusting the pore space on the surface of the electrode material, thus increasing the energy density. The low melting point, hydrophobicity and high purity of IL create conditions for the long cycle life of high-voltage supercapacitor [121, 137, 138]. The high ionic diffusivity of ILs can improve the contact angle between the electrode material and the electrolyte and thus improve the wettability of the electrode.

Electrodes, as another important component of ECs, are the core of control the performance and function of supercapacitors [139]. Conventional electrodes mostly use carbon-based materials, such as activated carbon, carbon nanotubes, reduced graphene oxides, and templated carbon [140–142]. However, heteroatoms and micropores in commonly used electrode materials are uncontrollable. Hao *et al.* [143] constructed a 2D microporous covalent triazine structure (m-CTF) consisting of defined heteroatoms and/or pore size distributions, using $EMIMBF_4$ IL as the electrolyte to obtain a PTF-700 based supercapacitor. At a working voltage of 3 V, the supercapacitor obtained the highest energy density and power density of 47.4 Wh/kg and 7500 W/kg respectively, which are comparable to state-of-the-art systems reported in literatures [144–154]. Besides enhanced energy densities, pseudocapacitive storage at the surface of electrode materials can in principle be increased by involving redox species dissolved in the electrolyte [155–157]. A nanoporous carbon electrodes with matching electrolytes had proven to minimize self-discharge due to the desolvation of redox species in the pores. Even though the self-diffusion coefficient in confined pores had decreased by two orders of magnitude, the ion transport was still fast enough to ensure the high electrochemical energy storage [158]. Therefore, novel nanostructured electrode materials and suitable electrolytes may meet the needs of future generations of electronic devices [159]. In the following, we focus on the IL-modified 2D electrodes

in representative graphene, MXenes and MOFs systems.

Graphene has a large intrinsic carrier mobility (~200 000 $cm^2 \cdot V^{-1} \cdot s^{-1}$), high mechanical strength (Young's modulus ~1 TPa), and very high electrical conductivity (~10^6 $S \cdot cm^{-1}$) and high theoretical specific surface area (2630 $m^2 \cdot g^{-1}$), which is considered as a promising electrode material for ECs [21, 33, 160–162]. However, due to the strong van der Waals attraction between parallel graphene sheets, aggregation or restacking of graphene is unavoidable [163]. Notably, in IL electrolytes, porous and dense graphene gel films can be compressed by capillaries, achieving sub-nanoscale integration of graphene sheets with continuous ion transport networks [164]. The capillary-like forces between graphene and IL electrolytes can operate in two strategies. On the one hand, by adapting the pore sizes on graphene electrodes to that of the electrolyte ions, the local Coulomb order between graphene layers is disrupted when the ions are confined by the monolayer, which will be more efficient for charge storage [165–167]. On the other hand, a suitable contact-angle between electrode and electrolyte can improve the wettability of the electrode and the ion-diffusion properties. Wang *et al.* [163] made the porous structure in highly crumpled and nitrogen-doped graphene (CNG), which shows a contact angle is ~20° (versus 69° for non-doping Graphene electrode), as shown in Fig. 4(a). The CNG electrode exhibited enhanced electronic and ion transfer properties as well as excellent EC performance. Furthermore, heterogeneous structures with differential pore concentrations can facilitate higher capacitances. Su *et al.* [168] used activated carbon YP50F, reduced graphene oxide (rGO), and activated microwave exfoliated graphene oxide (aMEGO) with different pore characteristics as heterogeneous electrodes. By rational designing the stacking order of the electrode, the ion transport from the electrolyte can be optimized. When the rGO with the largest mesopores being placed in the middle, the device exhibited the higher capacitances (171.4 $F \cdot g^{-1}$, 102.8 $F \cdot cm^{-3}$, 2.2 $F \cdot cm^{-2}$) compared to other stacking orders or single types of electrodes at a voltage of 2.7 V using $EMIBF_4$/AN IL electrolyte. This strategy may open up more opportunities to improve supercapacitors with thicker or high-quality load electrodes.

In addition, IL can also form composites with 2D graphene nanosheets (GNS) which modifies the structural and electronic properties of graphene. Kim *et al.* [169] reported the preparation of GNS/IL composites simply by adding the IL([BMIM][PF_6]) in graphite oxide (GO) suspension prior to reduction procedure of GO into graphene. Dur to the stronger structural stability and the higher charge transfer of modified graphene, the GNS/IL composites exhibited higher specific capacitance of 114 $F \cdot g^{-1}$ and good rate capability (66% retention at 100 $mV \cdot s^{-1}$) compared to 99 $F \cdot g^{-1}$ and 37% retention of pristine GNS. The GNS/IL composites also showed enhanced cycle performance of ~80% retention of initial value for 3000 cycles (versus 45% retention of pristine GNS). Furthermore, the microstructure and capacitance of modified electrode were also dependent on the ILs concentration. In the rGO/IL composites, the IL([BMIM][PF_6]) act as a medium for exfoliation of reduced graphene oxide sheets, the rGO/IL (1:7) composite exhibited better rate capability by retaining 55% of the initial capacitance at 300 $mV \cdot s^{-1}$ compared to 11.5% for pristine rGO. The increased specific capacitance and rate capability of the rGO/IL composites can be ascribed to the modification of the surface of rGO sheets by IL [170].

MXenes have good electrical conductivity and are currently being investigated as anodes for battery and supercapacitor applications, as well as in hydrogen storage and adsorbents [171–178]. However, MXene electrode-based micro-supercapacitors [179, 180] exhibit low area (≤10 $\mu W \cdot h \cdot cm^{-2}$) and volumetric (≤20 $mW \cdot h \cdot cm^{-3}$) energy densities due to their narrow working voltage in aqueous systems (typically, 0.6–1.0 V). Using IL electrolyte, the voltage window can be increased. In pure (1-ethyl-3-methylimidazolium bis(trifluoromethylsulfonyl) imide (EMI-TFSI)) IL electrolyte [181], it was found that the $Ti_3C_2T_x$ surface became susceptible to different cations and/or anions of the IL electrolyte under different polarizations. The $Ti_3C_2T_x$ MXene achieved a capacitance of 70 $F \cdot g^{-1}$ with a large voltage window of 3 V at a scan rate of 20 $mV \cdot s^{-1}$.

Moreover, the electrostatic attraction effect generated between the ions in the IL and the MXene nanosheets can also contribute to the regulation of the interlayer spacing of the nanosheets [182]. Benefitting from the pre-intercalation of ILs [183], MXene-based electrode films prepared by interdigitated mask-assisted deposition of MXene and grapheme [183], exhibited continuously developed ion transport network with interlayer spacing of 1.45 nm, as shown in Fig. 4(b). This spacing is larger than that of the fresh undried MXene (1.27 nm) and fully dried MXene (1.09 nm). The resulting micro-supercapacitors (MSCs) assembled with the $EMIMBF_4$ pre-intercalated films and tested in the same electrolyte of $EMIMBF_4$, delivering a remarkably high volumetric capacitance of 140 $F \cdot cm^{-3}$, high areal and volumetric energy density of 13.9 $\mu W \cdot h \cdot cm^{-2}$ and 43.7 $mW \cdot h \cdot cm^{-3}$, as well as a long-term cyclability up to 10 000 cycles. The energy density values are the highest of the state-of-the-art MXene based MSCs reported.

The alkyl chain length of the IL cation has also been used to modulate the interlayer spacing of MXene [184]. Naguib *et al.* [185] tried to use different chain lengths alkylammonium (AA) cations as intercalation layers into $Ti_3C_2T_x$, in order to produce variation of MXene interlayer spacings (d-spacing), as shown in Fig. 4(c). AA-cation-intercalated $Ti_3C_2T_x$ (Ti_3C_2-AA) displayed an enhanced interlayer of ~2.2 nm and exhibited higher specific capacitances and cycling stabilities than these of pristine $Ti_3C_2T_x$ in 1 M 1-ethly-3-methylimidazolium bis-(trifluoromethylsulfonyl)-imide (EMIM-TFSI) in acetonitrile and neat EMIM-TFSI RTIL electrolytes. Fan *et al.* [186]

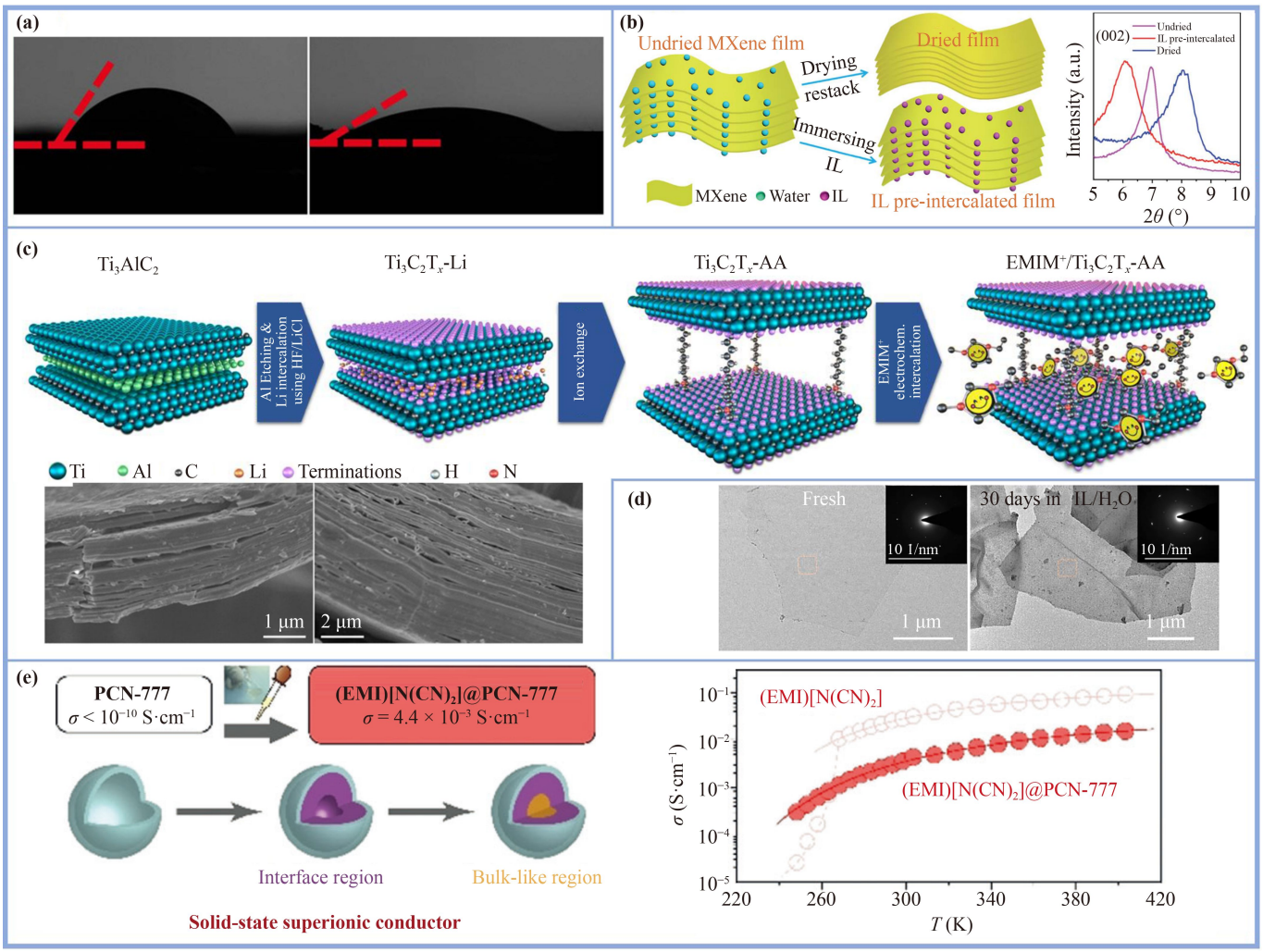

Fig. 4 **(a)** The CNG surface was subjected to wetting by the IL electrolyte for contact angle testing, and the CNG showed a more hydrophilic surface with a contact angle of 20° (right) (compared to 69° (left) for the GS) allowing wetting of previously inaccessible pores. Reprinted with permission from Ref. [163], Copyright © 2015 ACS Applied Materials & Interfaces. **(b)** The preparation schematic of IL pre-intercalated MXene films for ionogel-based flexible micro-supercapacitors with high volumetric energy density. The XRD patterns show the intercalated MXene film with enhanced interlayer spacing of 1.45 nm. Reprinted with permission from Ref. [183], Copyright © 2019 Journal of Materials Chemistry A. **(c)** Alkylammonium (AA) cations with different chain lengths were intercalated into $Ti_3C_2T_x$, producing different degrees of MXene interlayer spacing (d-spacing). Compared with the pristine $Ti_3C_2T_x$, the AA cation intercalated $Ti_3C_2T_x$ (Ti_3C_2-AA) exhibits higher specific capacitance and cycling stability. Top image shown a schematic for the preparation of $Ti_3C_2T_x$-AA and intercalation of $EMIM^+$. And SEM images of (left) pristine $Ti_3C_2T_x$ and (right) alkylammonium cations intercalated $Ti_3C_2T_x$ materials. Reprinted with permission from Ref. [185], Copyright © 2021 Advanced Functional Materials. **(d)** The modification with imidazolium-based ILs protected the sensitive $Ti_3C_2T_x$ from degradation, significantly improved the chemical stability of $Ti_3C_2T_x$ in aqueous solution, shown as the TEM images and the corresponding SAED pattern of fresh MXene (left) and IL-MXene flakes (right). IL can postpone the degradation of $Ti_3C_2T_x$ MXene sheets in aqueous solution. Reprinted with permission from Ref. [187], Copyright © 2021 Chemical Engineering Journal. **(e)** The solid-state superionic conductor was obtained by incorporating IL into MOF. The hybrid shows the highest room temperature conductivity (4.4×10^{-3} S·cm^{-1}) among the IL-inorporated MOF hybrids reported so far. Schematic of solid-state superionic conductor and room temperature conductivity of IL-inorporated MOF hybrid. Reprinted with permission from Ref. [189], Copyright © 2019 Angewandte Chemie-International Edition.

introduced polymerized polypyrrole (PPy) particles and ILs -based microemulsion particles as "double spacers" to prepare high-performance functionalized $Ti_3C_2T_x$ MXene composite films. Specifically, the as-prepared PPy-MXene-IL-mic ($[EIm][NTf_2]$) or ($[EMIM][NTf_2]$) composite film can achieve a high gravimetric capacitance of 51.85 F·g^{-1} at a scan rate of 20 mV·s^{-1} and a temperature range between 4 and 50 °C. Moreover, the symmetric

supercapacitor device based on the composite films exhibited a maximum gravimetric energy density of 31.2 $Wh \cdot kg^{-1}$ (at 1030.4 $W \cdot kg^{-1}$) at room temperature, as well as 91% retention of the initial specific capacitance after 2000 cycles while coulombic efficiency is 91%.

Another fundamental challenge limiting the implementation of $Ti_3C_2T_x$ in practical applications is its susceptibility to oxidation in humid or aqueous environments within only a few days, leading to severely deteriorates of the electrical conductivity characteristics, mechanical strength and EMI shielding performance [187]. Wan *et al.* [187] protected sensitive $Ti_3C_2T_x$ from degradation by imidazolium-based IL modification, which significantly improved the chemical stability of $Ti_3C_2T_x$ in aqueous solution and the assembled free-standing $Ti_3C_2T_x$ thin films (IL-MXene) , as shown in Fig. 4(d). The crystal structure of the IL-MXene sheet remained intact for up to 30 days and the 2D layered structure in aqueous solution for up to 8 months, while the tensile strength of the free-standing IL-MXene film was as high as 75.9±4.9 MPa and comparable to that of untreated IL-MXene films. Compared with the treated MXene film (41.2±4.5 MPa), the increased tensile strength is as high as 84%. Based on the radical scavenging ability of IL and the surface chemistry of MXene sheets, a new mechanism to improve the chemical stability of MXene sheets is proposed and elucidated.

In another group of 2D electrode material, i.e., 2D MOFs, adding a small amount of ILs with good thermal stability and high ionic conductivity into MOFs can efficiently overcome one of the main disadvantages of MOFs, namely the low ionic conductivity of MOFs at room temperature [188]. Yoshida *et al.* [189] investigated the relationship between the radial distribution and the ion conductivity of the hybrid system in the hole through exploring the relevant characteristics of the mesoporous MOFs containing different filling levels, as shown in Fig. 4(e). The result showed that the ions with high mobility occupying the bulk-like region led to a new class of solid-state superionic conductors with the highest σ_{298K} (4.4×10^{-3} $S \cdot cm^{-1}$) among the IL-incorporated MOF hybrids reported up to date. Furthermore, the hybrid system exhibited a notable ionic conduction over a wide temperature range. The σ value steadily increases up to ca. 400 K (>10^{-2} $S \cdot cm^{-1}$ above 343 K) and exceeds that of the parent IL at low temperatures (<263 K). Such special features make it a promising green and versatile alternative to conventional aqueous electrolytes over a wide temperature range across room temperature. Feng *et al.* [190] analyzed the microstructure of room temperature ILs in MOF pores from the perspective of in-plane (2D) and axial (1D) ion distribution and ion orientation, elucidating how ions transport and reside within polarized porous MOFs. The results revealed that these MOF/RTIL-based cells could exhibit performance superior to most carbon-based devices [128, 164, 191–193], which suggested promising avenues for designing supercapacitors with both high energy and high power densities. In addition to changing the MOFs electrode mobility, adding aqueous electrolytes or organic electrolytes can also improve the low mobility problem caused by the high viscosity of ILs [194–199].

6 IL enhanced perovskite crystallization in photovoltaic cell

Halide perovskites have outstanding performance in optoelectronic applications due to their high absorption coefficient, high carrier mobility, and tunable direct bandgap [200]. However, various defects can be formed due to the precursor composition and processing conditions, as well as the rapid growth rate of perovskite thin films. Ion migration in the perovskite active layer — especially under illumination and heat — is arguably the most difficult aspect to mitigate [201–204]. The wide band gap, anti-reflection, high electron mobility and suitable work function characteristics of ILs can reduce the ion migration, control the crystallization of perovskite films and decrease the structural defects at the passivation interface. It is shown that the abundant free ion pairs in IL can combine with ions on the perovskite surface, thus effectively passivating the structural defects at the interface and improving ion migration. Bai *et al.* [201] added [BMIM][BF_4] ILs to perovskite films and found that the work function of the chalcogenide films decreased from 5.13 eV with the addition of $BMIMBF_4$ to 4.81 eV, and the energy level of the perovskite absorber is close to vacuum. The change in energy level structure is mainly due to the accumulation of ion pairs of BMIM and BF_4 at the perovskite/NiO interface. The interactions between chalcogenide and NiO at the interface are promoted, thus enhancing the performance and efficiency of the device. Specifically, it was observed that the performance of the most stable encapsulated device degraded by only about 5% after 1800 hours of continuous simulation of full-spectrum sunlight at 70 to 75 degrees Celsius. The time required for the device to degrade to 80% of its peak performance was estimated to be about 5200 hours. This is a critical step toward reliable encapsulated PV technology [201]. Zhu *et al.* [205] used 1,3-dimethyl-3-imidazolium [PF_6] ($DMIMPF_6$) (IL) to passivate the surface energy of $Cs_{0.08}FA_{0.92}PbI_3$, which simultaneously lowered the energy barrier between the perovskites film layer and hole transport layer. Theoretical simulations and experimental results show that the Pb-cluster and Pb-I antisite defects can be effectively passivated by [DMIM] bonding with Pb^{2+} ions on the perovskite surface, thereby significantly suppressing nonradiative recombination. As a result, the solar cell efficiency increased

from 21.09% to 23.25%. Meanwhile, $DMIMPF_6^-$ treated perovskite devices exhibited long-term stability because of the preventing of moisture penetration by hydrophobic $DMIMPF_6$ layer. In other studies, ILs had been used as additives in perovskite precursor solutions to ensure maximum device lifetime under constant illumination [206]. In addition, based on the excellent thermoelasticity of IL [207], [BMI] IL was employed as an organic spacer in 2D perovskite to fundamentally change the quantum well structure, the synthesized perovskite solar cells exhibited extraordinary thermal stability under 85 °C aging. Hui *et al.* [208] reported an alternative route in which vertically aligned lead iodide thin films were grown from the methylamine IL formate. Nanoscale channels in the films lowered the barrier to permeation of formamidinium iodide and enabled transformation to α-$FAPbI_3$, even at high humidity and room temperature. Solar cells made with these films possessed power conversion efficiencies as high as 24.1% and high stability.

7 ILs encapsuled 2D photocatalyst

It is well known that nanostructured semiconductors have strong environmental remediation capabilities [209], and ultrathin 2D materials with suitable band gaps are ideal materials for high-performance photocatalytic applications [210–212]. Ultrathin structural material can transport charge carriers inside the material to the surface extremely quickly, thereby promoting photocatalytic activity [213]. Among them, bismuth oxyhalide, as a novel layered material with broad spectral response, has excellent photocatalytic performance [214, 215]. It is demonstrated that efficient two-dimensional bismuth oxyhalide photocatalytic systems can be modified through size and structure control of the surface, while ILs can promote the growth of photocatalysts composed of isolated few-layer or single-layer nanosheets [216–219]. In addition, the non-metallic doping of organic cations in ILs also affects the photoactivity of 2D photocatalysts in the reaction environment. [N-methyl-pyrrolidonium] chloride IL can enhance solvothermal process and act as carbon source for $Bi_2O_2CO_3$ [220]. β-Bi_2O_3/$Bi_2O_2CO_3$ is obtained via an IL-assisted solvothermal and calcination route, which has higher transfer ability of carriers and high activity in visible-light. The IL acts as an intercalating and stabilizing agent in addition to being an efficient solvent for the synthesis of few-layer Bi_2Se_3 [221], the ionothermal reaction of bismuth acetate and selenourea in [EMIM][BF_4] yields ultrathin (3–5 layer) Bi_2Se_3 nanostructures. Similarly, a novel visible light-driven g-C_3N_4/$Bi_4O_5Br_2$ composite was prepared by the 1-hexadecyl-3-methylimidazole bromide ([C16mim]Br)IL-assisted solvothermal method [222]. Chen *et al.* [223] determined that Bi_2MoO_6 nanosheets can be controlled by ILs with ammonium cation alkyl chain lengths and polar anions, and their adsorption capacities for azo molecules are in good agreement with the σ-profiles obtained from conductor-like screening models for realistic solvents. Pancielejko *et al.* [224] found that the amount of IL was beneficial to control the thickness and photoactivity of the nanosheets, and the obtained ultrathin IL_Bi_2WO_6 improved activity with h^+ and ·OH dominating role in phenol degradation. Meanwhile, it is speculated that in view of the tunable nature and antimicrobial qualities of ILs-assisted photocatalyst, the presence of IL residues could affect for an enhanced inactivation Gram-negative and Gram-positive bacterium [224].

8 Conclusions and perspectives

In conclusion, ILs as new environmentally friendly chemical solvents, can be designed with different combination of cations and anions or ionic chain lengths, showing rich applications in chemistry, physics, energy science, materials science, etc. This article focuses on the multiple applications of ILs in 2D material systems. Due to their highly ionic nature, ILs interact strongly with nanoparticles, which in turn promotes the formation of well-defined layered structures on the charged surfaces of nanocrystals. We present the usage of ILs for exfoliation and stabilization of 2D ultrathin nanosheets, where the physical properties of ILs can further facilitate the functionalization of 2D nanosheet. Moreover, the usage of IL shows advantage to obtain defect-free single-layer or few layers of graphene with large area and smooth edges due to the strong interaction between the π electron cloud of imidazole cation in ILs with various π electron in carbon nanomaterials. This implies potentials in exfoliation other defect-free 2D materials using ILs [68, 70, 76, 89, 225]. Furthermore, ILs with high ionic concentration have shown as an efficient tuning manner to induce novel physical properties, such as insulator-metal transition, unconventional superconductivity and quantum phase transitions, through electric-field controlled IL-gating.

Besides the fundamental scientific interests on ILs, ILs have been largely applied in energy storage fields, and we review the applications in the fields of ECs, solar cells and photocatalysis. Regarding ECs field, IL-based electrolytes allow an increased electrochemical voltage window of 4–6 V. ILs can also modify the electrodes in terms of controlling the capillary-like forces between the IL electrolytes and 2D electrodes or forming the composites. ILs as the intercalation layer can also increase the interlayer spacing of 2D nanosheets. By adjusting the pore size or the alkyl chain length of the electrolyte ions, the interlayer spacing can be engineered, resulting in better energy storage properties. Moreover, the environ-

ment and structure stability can be protected by ILs. Halide perovskites show outstanding performance but easier formations of various defects during perovskite film growth. ILs exhibit promising potentials in controlling the crystallization of perovskite films, reducing ion migration and passivating certain defects. In 2D photocatalyst aspect, ILs can not only modify the size and structure of the surface, but also modulate the photoactivity through the non-metallic doping of organic cations from ILs.

ILs have also shown promising applications as the intercalation and dispersion media in 1D and 0D systems [226]. Moreover, ILs can be designed with tunable properties, which provides more possibilities for different purposes. Even the mixture of ILs with different fractions of water can be engineered for the exfoliation of 2D nanosheet, which affects the viscosity, electrical conductivity as well as the complex Coulomb, van der Waals, hydrogen bonding, and π-π interactions therein [227]. At present, the applications of ILs in the field of 2D materials is only in the initial stage, and there are many possibilities for future modulations at the microscopic level.

In recent years, with people's increasing attention to their own health and environmental issues, the design of stable, efficient and processable bactericidal materials is a major challenge in various engineering fields against multi drug resistant bacteria [228–231]. Zhang *et al.* [228] also proposed in recent hot articles that the nano spheres with excellent antibacterial activity will be loaded with imidazole based ionic liquids, which has achieved good biocompatibility and made outstanding contributions to the bactericidal application in the field of biomedical activity. In addition, the combination of ILs and other nanomaterials for the joint detection of colorants in food and cosmetics has also become a research hotspot in recent two years. It is believed that the combination of ILs and 2D materials will create more contributions in the future [232, 233].

Acknowledgements This work was supported by the Natural Science Foundation of Fujian Province of China (No. 2022J01007), the Fundamental Research Funds for Central Universities (Grant No. 20720210018), and the National Natural Science Foundation of China (No. 11704317).

Abbreviations

Cations of ILs	
[BMIM]	1-butyl-3-methylimidazolium
[EMIM]	1-ethyl-3-methylimidazolium

Anions of ILs	
[PF_6]	hexafluorophosphate
[BF_4]	tetrafluoroborate
[TFSI] or [NTf_2]	bis(trifluoromethylsulfonyl) imide

Other	
ILs	Ionic liquids
2D materials	two-dimensional materials
TMDs	transition metal dichalcogenide
MoS_2	molybdenum disulfide
$MoSe_2$	Molybdenum(IV) selenide
$MoTe_2$	Molybdenum Ditelluride
WS_2	Tungsten disulfide
WSe_2	Tungsten(IV) selenide
ReS_2	Rhenium Disulfide
TaS_2	tantalum disulfide
NMDs	noble metal dichalcogenides
$PdSe_2$	Palladium diselenide
$PtSe_2$	Platina Diselenide
PtS_2	Platinum disulfide
h-BN	hexanol boron nitride
BP	black phosphorus
LDHs	layered double hydroxide
g-C_3N_4	graphite carbon nitrides
MOFs	metal-organic frameworks
COFs	covalent-organic frameworks
LPE	liquid phase exfoliation
NMP	N-methylpyrrolidone
N12P	1-dodecyl-2-pyrrolidone
(P[VBTP][Cl])	poly(triphenyl-4-vinylbenzylphosphonium chloride)
(P[VimBu][Br])	poly(3-N-butyl-1-vinylimidazolium bromide)
(PNIL)	(poly(*N*-isopropylacrylamide-co-IL)
FG	fluorinated graphene
EDLTs	electrical double-layer transistors
FETs	field-effect transistors
CNT	carbon nanotubes
SS	subthreshold swing
CDW	charge-density-wave
$Cr_2Ge_2Te_6$	Chromium germanium tellurium
m-CTF	microporous covalent triazine structure
rGO	reduced graphene oxide
aMEGO	activated microwave exfoliated graphene oxide
GNS	2D graphene nanosheets
GO	graphite oxide
(EMI-TFSI)	1-ethyl-3-methylimidazolium bis(trifluoromethylsulfonyl) imide
$Ti_3C_2T_x$	Titanium carbide
MSCs	micro-supercapacitors
AA-Ti_3C_2	AA-cation-intercalated $Ti_3C_2T_x$
EMIM-TFSI	1-ethly-3-methylimidazolium bis-(trifluoromethylsulfonyl)-imide
DMIM	1,3-dimethyl-3-imidazolium
$Cs_{0.08}FA_{0.92}PbI_3$	formamidinium-cesium lead iodide perovskite
[Hnmp]Cl	[N-methyl-pyrrolidonium] chloride
$Bi_2O_2CO_3$	Bismuth subcarbonate
Bi_2Se_3	bismuth selenide
[C16mim]Br	1-hexadecyl-3-methylimidazole bromide
Bi_2MoO_6	Bismuth molybdenum oxide
Bi_2WO_6	Bismuth tungstate

References

1. T. Welton, Room-temperature ionic liquids: Solvents for synthesis and catalysis, *Chem. Rev.* 99(8), 2071 (1999)
2. J. P. Hallett and T. Welton, Room-temperature ionic liquids: Solvents for synthesis and catalysis. 2, *Chem. Rev.* 111(5), 3508 (2011)
3. S. K. Singh and A. W. Savoy, Ionic liquids synthesis and applications: An overview, *J. Mol. Liq.* 297, 112038 (2020)
4. K. S. Egorova, E. G. Gordeev, and V. P. Ananikov, Biological activity of ionic liquids and their application in pharmaceutics and medicine, *Chem. Rev.* 117, 7132 (2017)
5. J. M. Gomes, S. S. Silva, and R. L. Reis, Biocompatible ionic liquids: Fundamental behaviours and applications, *Chem. Soc. Rev.* 48(15), 4317 (2019)
6. D. R. MacFarlane, M. Forsyth, P. C. Howlett, M. Kar, S. Passerini, J. M. Pringle, H. Ohno, M. Watanabe, F. Yan, W. J. Zheng, S. G. Zhang, and J. Zhang, Ionic liquids and their solid-state analogues as materials for energy generation and storage, *Nat. Rev. Mater.* 1(2), 15005 (2016)
7. W. J. Zhou, M. Zhang, X. Y. Kong, W. W. Huang, and Q. C. Zhang, Recent advance in ionic-liquid-based electrolytes for rechargeable metal-ion batteries, *Adv. Sci. (Weinh.)* 8(13), 2004490 (2021)
8. L. Li, N. Zhao, W. Wei, and Y. H. Sun, A review of research progress on CO_2 capture, storage, and utilization in Chinese Academy of Sciences, *Fuel* 108, 112 (2013)
9. X. X. Tan, X. F. Sun, and B. X. Han, Ionic liquid-based electrolytes for CO_2 electroreduction and CO_2 electroorganic transformation, *Natl. Sci. Rev.* 9(4), nwab022 (2022)
10. E. V. Kondratenko, G. Mul, J. Baltrusaitis, G. O. Larrazabal, and J. Perez-Ramirez, Status and perspectives of CO_2 conversion into fuels and chemicals by catalytic, photocatalytic and electrocatalytic processes, *Energy Environ. Sci.* 6(11), 3112 (2013)
11. A. J. Greer, J. Jacquemin, and C. Hardacre, Industrial applications of ionic liquids, *Molecules* 25 (2020)
12. N. Nasirpour, M. Mohammadpourfard, and S. Z. Heris, Ionic liquids: Promising compounds for sustainable chemical processes and applications, *Chem. Eng. Res. Des.* 160, 264 (2020)
13. A. A. Elgharbawy, F. A. Riyadi, M. Z. Alam, and M. Moniruzzaman, Ionic liquids as a potential solvent for lipase-catalysed reactions: A review, *J. Mol. Liq.* 251, 150 (2018)
14. J. C. Cui, Y. Li, D. Chen, T. G. Zhan, and K. D. Zhang, Ionic liquid-based stimuli-responsive functional materials, *Adv. Funct. Mater.* 30(50), 2005522 (2020)
15. C. W. Cho, T. P. T. Pham, Y. F. Zhao, S. Stolte, and Y. S. Yun, Review of the toxic effects of ionic liquids, *Sci. Total Environ.* 786, 147309 (2021)
16. X. C. Duan, H. Huang, S. H. Xiao, J. W. Deng, G. Zhou, Q. H. Li, and T. Wang, 3D hierarchical CuO mesocrystals from ionic liquid precursors: Towards better electrochemical performance for Li-ion batteries, *J. Mater. Chem. A* 4(21), 8402 (2016)
17. R. D. Rogers and K. R. Seddon, Ionic liquids - Solvents of the future, *Science* 302(5646), 792 (2003)
18. A. K. Geim and K. S. Novoselov, The rise of graphene, *Nat. Mater.* 6(3), 183 (2007)
19. W. Kong, H. Kum, S. H. Bae, J. Shim, H. Kim, L. P. Kong, Y. Meng, K. J. Wang, C. Kim, and J. Kim, Path towards graphene commercialization from lab to market, *Nat. Nanotechnol.* 14(10), 927 (2019)
20. K. S. Novoselov, A. Mishchenko, A. Carvalho, and A. H. Castro Neto, 2D materials and van der Waals heterostructures, *Science* 353(6298), aac9439 (2016)
21. S. Mukherjee, Z. Ren, and G. Singh, Beyond graphene anode materials for emerging metal ion batteries and supercapacitors, *Nano-Micro Lett.* 10(4), 70 (2018)
22. S. Jo, N. Ubrig, H. Berger, A. B. Kuzmenko, and A. F. Morpurgo, Mono- and bilayer WS_2 light-emitting transistors, *Nano Lett.* 14(4), 2019 (2014)
23. V. Podzorov, M. E. Gershenson, C. Kloc, R. Zeis, and E. Bucher, High-mobility field-effect transistors based on transition metal dichalcogenides, *Appl. Phys. Lett.* 84(17), 3301 (2004)
24. Y. Zhang, J. Ye, Y. Matsuhashi, and Y. Iwasa, Ambipolar MoS_2 thin flake transistors, *Nano Lett.* 12(3), 1136 (2012)
25. D. Braga, I. G. Lezama, H. Berger, and A. F. Morpurgo, Quantitative determination of the band gap of WS_2 with ambipolar ionic liquid-gated transistors, *Nano Lett.* 12(10), 5218 (2012)
26. A. Splendiani, L. Sun, Y. Zhang, T. Li, J. Kim, C. Y. Chim, G. Galli, and F. Wang, Emerging photoluminescence in monolayer MoS_2, *Nano Lett.* 10(4), 1271 (2010)
27. K. F. Mak, C. Lee, J. Hone, J. Shan, and T. F. Heinz, Atomically thin MoS_2: A new direct-gap semiconductor, *Phys. Rev. Lett.* 105(13), 136805 (2010)
28. A. Kumar, and P. K. Ahluwalia, Electronic structure of transition metal dichalcogenides monolayers 1H-MX_2 (M = Mo, W; X = S, Se, Te) from *ab-initio* theory: New direct band gap semiconductors, *Eur. Phys. J. B* 85(6), 186 (2012)
29. Y. Chen, J. Xi, D. O. Dumcenco, Z. Liu, K. Suenaga, D. Wang, Z. Shuai, Y. S. Huang, and L. Xie, Tunable band gap photoluminescence from atomically thin transition-metal dichalcogenide alloys, *ACS Nano* 7(5), 4610 (2013)
30. H. Terrones, F. Lopez-Urias, and M. Terrones, Novel hetero-layered materials with tunable direct band gaps by sandwiching different metal disulfides and diselenides, *Sci. Rep.* 3(1), 1549 (2013)
31. Y. Zhang, M. Jeon, L. J. Rich, H. Hong, J. Geng, Y. Zhang, S. Shi, T. E. Barnhart, P. Alexandridis, J. D. Huizinga, M. Seshadri, W. Cai, C. Kim, and J. F. Lovell, Non-invasive multimodal functional imaging of the intestine with frozen micellar naphthalocyanines, *Nat. Nanotechnol.* 9(8), 631 (2014)
32. A. K. Geim and K. S. Novoselov, The rise and rise of graphene, *Nat. Nanotechnol.* 5(11), 755 (2010)
33. C. Lee, X. D. Wei, J. W. Kysar, and J. Hone, Measurement of the elastic properties and intrinsic

strength of monolayer graphene, *Science* 321(5887), 385 (2008)
34. A. H. Castro Neto, F. Guinea, N. M. R. Peres, K. S. Novoselov, and A. K. Geim, The electronic properties of graphene, *Rev. Mod. Phys.* 81(1), 109 (2009)
35. L. Song, L. J. Ci, H. Lu, P. B. Sorokin, C. H. Jin, J. Ni, A. G. Kvashnin, D. G. Kvashnin, J. Lou, B. I. Yakobson, and P. M. Ajayan, Large scale growth and characterization of atomic hexagonal boron nitride layers, *Nano Lett.* 10(8), 3209 (2010)
36. J. C. Zheng, L. Zhang, A. V. Kretinin, S. V. Morozov, Y. B. Wang, T. Wang, X. J. Li, F. Ren, J. Y. Zhang, C. Y. Lu, J. C. Chen, M. Lu, H. Q. Wang, A. K. Geim, and K. S. Novoselov, High thermal conductivity of hexagonal boron nitride laminates, *2D Mater.* 3, 011004 (2016)
37. L. K. Li, Y. J. Yu, G. J. Ye, Q. Q. Ge, X. D. Ou, H. Wu, D. L. Feng, X. H. Chen, and Y. B. Zhang, Black phosphorus field-effect transistors, *Nat. Nanotechnol.* 9(5), 372 (2014)
38. L. Tao, E. Cinquanta, D. Chiappe, C. Grazianetti, M. Fanciulli, M. Dubey, A. Molle, and D. Akinwande, Silicene field-effect transistors operating at room temperature, *Nat. Nanotechnol.* 10(3), 227 (2015)
39. S. Balendhran, S. Walia, H. Nili, S. Sriram, and M. Bhaskaran, Elemental analogues of graphene: Silicene, germanene, stanene, and phosphorene, *Small* 11(6), 640 (2015)
40. Z. Q. Wang, T. Y. Lu, H. Q. Wang, Y. P. Feng, and J. C. Zheng, Review of borophene and its potential applications, *Front. Phys.* 14(3), 33403 (2019)
41. W. J. Ong, L. L. Tan, Y. H. Ng, S. T. Yong, and S. P. Chai, Graphitic carbon nitride ($g\text{-}C_3N_4$)-based photocatalysts for artificial photosynthesis and environmental remediation: Are we a step closer to achieving sustainability, *Chem. Rev.* 116(12), 7159 (2016)
42. J. B. Pang, R. G. Mendes, A. Bachmatiuk, L. Zhao, H. Q. Ta, T. Gemming, H. Liu, Z. F. Liu, and M. H. Rummeli, Applications of 2D MXenes in energy conversion and storage systems, *Chem. Soc. Rev.* 48(1), 72 (2019)
43. K. Khan, A. K. Tareen, M. Aslam, Y. P. Zhang, R. H. Wang, Z. B. Ouyang, Z. Y. Gou, and H. Zhang, Recent advances in two-dimensional materials and their nanocomposites in sustainable energy conversion applications, *Nanoscale* 11(45), 21622 (2019)
44. X. L. Chen, Z. S. Zhou, B. C. Deng, Z. F. Wu, F. N. Xia, Y. Cao, L. Zhang, W. Huang, N. Wang, and L. Wang, Electrically tunable physical properties of two-dimensional materials, *Nano Today* 27, 99 (2019)
45. Y. Liu, N. O. Weiss, X. D. Duan, H. C. Cheng, Y. Huang, and X. F. Duan, Van der Waals heterostructures and devices, *Nat. Rev. Mater.* 1(9), 16042 (2016)
46. C. S. Liu, H. W. Chen, S. Y. Wang, Q. Liu, Y. G. Jiang, D. W. Zhang, M. Liu, and P. Zhou, Two-dimensional materials for next-generation computing technologies, *Nat. Nanotechnol.* 15(7), 545 (2020)
47. K. Kang, S. E. Xie, L. J. Huang, Y. M. Han, P. Y. Huang, K. F. Mak, C. J. Kim, D. Muller, and J. Park, High-mobility three-atom-thick semiconducting films with wafer-scale homogeneity, *Nature* 520(7549), 656 (2015)
48. C. Chang, W. Chen, Y. Chen, Y. H. Chen, Y. Chen, et al., Recent progress on two-dimensional materials, *Acta Phys. - Chim. Sin.* 37(12), 2108017 (2021)
49. S. Keskin, D. Kayrak-Talay, U. Akman, and O. Hortacsu, A review of ionic liquids towards supercritical fluid applications, *J. Supercrit. Fluids* 43(1), 150 (2007)
50. A. Shariati and C. J. Peters, High-pressure phase equilibria of systems with ionic liquids, *J. Supercrit. Fluids* 34(2), 171 (2005)
51. J. F. Brennecke and E. J. Maginn, Ionic liquids: Innovative fluids for chemical processing, *AIChE J.* 47(11), 2384 (2001)
52. J. N. Coleman, M. Lotya, A. O'Neill, S. D. Bergin, P. J. King, et al., Two-dimensional nanosheets produced by liquid exfoliation of layered materials, *Science* 331(6017), 568 (2011)
53. S. Xu, D. Li, and P. Wu, One-pot, facile, and versatile synthesis of monolayer MoS_2/WS_2 quantum dots as bioimaging probes and efficient electrocatalysts for hydrogen evolution reaction, *Adv. Funct. Mater.* 25(7), 1127 (2015)
54. Y. Chen, C. Tan, H. Zhang, and L. Wang, Two-dimensional graphene analogues for biomedical applications, *Chem. Soc. Rev.* 44(9), 2681 (2015)
55. Q. H. Wang, K. Kalantar-Zadeh, A. Kis, J. N. Coleman, and M. S. Strano, Electronics and optoelectronics of two-dimensional transition metal dichalcogenides, *Nat. Nanotechnol.* 7(11), 699 (2012)
56. F. H. L. Koppens, T. Mueller, P. Avouris, A. C. Ferrari, M. S. Vitiello, and M. Polini, Photodetectors based on graphene, other two-dimensional materials and hybrid systems, *Nat. Nanotechnol.* 9(10), 780 (2014)
57. W. Luo, Y. Wang, E. Hitz, Y. Lin, B. Yang, and L. Hu, Solution processed boron nitride nanosheets: Synthesis, assemblies and emerging applications, *Adv. Funct. Mater.* 27(31), 1701450 (2017)
58. X. Wang, H. Feng, Y. Wu, and L. Jiao, Controlled synthesis of highly crystalline mos_2 flakes by chemical vapor deposition, *J. Am. Chem. Soc.* 135(14), 5304 (2013)
59. W. Xing, Y. Chen, X. Wu, X. Xu, P. Ye, T. Zhu, Q. Guo, L. Yang, W. Li, and H. Huang, PEDOT: PSS-assisted exfoliation and functionalization of 2D nanosheets for high-performance organic solar cells, *Adv. Funct. Mater.* 27(32), 1701622 (2017)
60. M. Yi and Z. Shen, A review on mechanical exfoliation for the scalable production of graphene, *J. Mater. Chem. A* 3(22), 11700 (2015)
61. Y. Hernandez, V. Nicolosi, M. Lotya, F. M. Blighe, Z. Sun, S. De, I. T. McGovern, B. Holland, M. Byrne, Y. K. Gun'ko, J. J. Boland, P. Niraj, G. Duesberg, S. Krishnamurthy, R. Goodhue, J. Hutchison, V. Scardaci, A. C. Ferrari, and J. N. Coleman, High-yield production of graphene by liquid-phase exfoliation of graphite, *Nat. Nanotechnol.* 3(9), 563 (2008)
62. L. Niu, J. N. Coleman, H. Zhang, H. Shin, M. Chhowalla, and Z. Zheng, Production of two-dimensional nanomaterials via liquid-based direct exfoliation, *Small*

12(3), 272 (2016)
63. H. Tao, Y. Zhang, Y. Gao, Z. Sun, C. Yan, and J. Texter, Scalable exfoliation and dispersion of two-dimensional materials — an update, *Phys. Chem. Chem. Phys.* 19(2), 921 (2017)
64. X. Feng, W. Xing, H. Yang, B. Yuan, L. Song, Y. Hu, and K. M. Liew, High-performance poly(ethylene oxide) /molybdenum disulfide nanocomposite films: Reinforcement of properties based on the gradient interface effect, *ACS Appl. Mater. Interfaces* 7(24), 13164 (2015)
65. R. D. Rogers, Reflections on ionic liquids, *Nature* 447(7147), 917 (2007)
66. W. Li and P. Wu, Unusual thermal phase transition behavior of an ionic liquid and poly(ionic liquid) in water with significantly different LCST and dynamic mechanism, *Polym. Chem.* 5(19), 5578 (2014)
67. T. Morishita, H. Okamoto, Y. Katagiri, M. Matsushita, and K. Fukumori, A high-yield ionic liquid-promoted synthesis of boron nitride nanosheets by direct exfoliation, *Chem. Commun. (Camb.)* 51(60), 12068 (2015)
68. M. Matsumoto, Y. Saito, C. Park, T. Fukushima, and T. Aida, Ultrahigh-throughput exfoliation of graphite into pristine "single-layer" graphene using microwaves and molecularly engineered ionic liquids, *Nat. Chem.* 7(9), 730 (2015)
69. W. C. Du, X. Q. Jiang, and L. H. Zhu, From graphite to graphene: Direct liquid-phase exfoliation of graphite to produce single- and few-layered pristine graphene, *J. Mater. Chem. A* 1(36), 10592 (2013)
70. D. Nuvoli, L. Valentini, V. Alzari, S. Scognamillo, S. B. Bon, M. Piccinini, J. Illescas, and A. Mariani, High concentration few-layer graphene sheets obtained by liquid phase exfoliation of graphite in ionic liquid, *J. Mater. Chem.* 21(10), 3428 (2011)
71. E. Bordes, B. Morcos, D. Bourgogne, J. M. Andanson, P. O. Bussière, C. C. Santini, A. Benayad, M. C. Gomes, and A. A. H. Pádua, Dispersion and stabilization of exfoliated graphene in ionic liquids, *Front Chem.* 7, 223 (2019)
72. X. G. Gu, Y. Zhao, K. Sun, C. L. Z. Vieira, Z. J. Jia, C. Cui, Z. J. Wang, A. Walsh, and S. D. Huang, Method of ultrasound-assisted liquid-phase exfoliation to prepare graphene, *Ultrason. Sonochem.* 58, 104630 (2019)
73. J. Restolho, J. L. Mata, and B. Saramago, On the interfacial behavior of ionic liquids: Surface tensions and contact angles, *J. Colloid Interface Sci.* 340(1), 82 (2009)
74. J. A. Harnisch and M. D. Porter, Electrochemically modulated liquid chromatography: An electrochemical strategy for manipulating chromatographic retention, *Analyst (Lond.)* 126(11), 1841 (2001)
75. S. K. Reed, O. J. Lanning, and P. A. Madden, Electrochemical interface between an ionic liquid and a model metallic electrode, *J. Chem. Phys.* 126(8), 084704 (2007)
76. X. Q. Wang, P. F. Fulvio, G. A. Baker, G. M. Veith, R. R. Unocic, S. M. Mahurin, M. F. Chi, and S. Dai, Direct exfoliation of natural graphite into micrometre size few layers graphene sheets using ionic liquids, *Chem. Commun. (Camb.)* 46(25), 4487 (2010)
77. H. Beneš, R. K. Donato, P. Ecorchard, D. Popelkova, E. Pavlova, D. Schelonka, O. Pop-Georgievski, H. S. Schrekker, and V. Stengl, Direct delamination of graphite ore into defect-free graphene using a biphasic solvent system under pressurized ultrasound, *RSC Adv.* 6(8), 6008 (2016)
78. A. Winchester, S. Ghosh, S. M. Feng, A. L. Elias, T. Mallouk, M. Terrones, and S. Talapatra, Electrochemical characterization of liquid phase exfoliated two-dimensional layers of molybdenum disulfide, *ACS Appl. Mater. Interfaces* 6(3), 2125 (2014)
79. Y. Biswas, M. Dule, and T. K. Mandal, Poly(ionic liquid)-promoted solvent-borne efficient exfoliation of MoS_2/$MoSe_2$ nanosheets for dual-responsive dispersion and polymer nanocomposites, *J. Phys. Chem. C* 121(8), 4747 (2017)
80. G. Guan, S. Zhang, S. Liu, Y. Cai, M. Low, C. P. Teng, I. Y. Phang, Y. Cheng, K. L. Duei, B. M. Srinivasan, Y. Zheng, Y. W. Zhang, and M. Y. Han, Protein induces layer-by-layer exfoliation of transition metal dichalcogenides, *J. Am. Chem. Soc.* 137, 6152 (2015)
81. R. J. Smith, P. J. King, M. Lotya, C. Wirtz, U. Khan, S. De, A. O'Neill, G. S. Duesberg, J. C. Grunlan, G. Moriarty, J. Chen, J. Wang, A. I. Minett, V. Nicolosi, and J. N. Coleman, Large-scale exfoliation of inorganic layered compounds in aqueous surfactant solutions, *Adv. Mater.* 23, 3944 (2011)
82. Z. Lei, Y. Zhou, and P. Wu, Simultaneous exfoliation and functionalization of $MoSe_2$ nanosheets to prepare "smart" nanocomposite hydrogels with tunable dual stimuli-responsive behavior, *Small* 12(23), 3112 (2016)
83. X. W. Wang and P. Y. Wu, Aqueous phase exfoliation of two-dimensional materials assisted by thermoresponsive polymeric ionic liquid and their applications in stimuli-responsive hydrogels and highly thermally conductive films, *ACS Appl. Mater. Interfaces* 10(3), 2504 (2018)
84. R. Tian, X. Jia, J. Yang, Y. Li, and H. Song, Large-scale, green, and high-efficiency exfoliation and noncovalent functionalization of fluorinated graphene by ionic liquid crystal, *Chem. Eng. J.* 395, 125104 (2020)
85. R. Gusain, H. P. Mungse, N. Kumar, T. R. Ravindran, R. Pandian, H. Sugimura, and O. P. Khatri, Covalently attached graphene-ionic liquid hybrid nanomaterials: Synthesis, characterization and tribological application, *J. Mater. Chem. A* 4(3), 926 (2016)
86. M. Li, A. S. Westover, R. Carter, L. Oakes, N. Muralidharan, T. C. Boire, H. J. Sung, and C. L. Pint, Noncovalent Pi–Pi stacking at the carbon electrolyte interface: Controlling the voltage window of electrochemical supercapacitors, *ACS Appl. Mater. Interfaces* 8(30), 19558 (2016)
87. W. Song, J. Yan, and H. Ji, Tribological performance of an imidazolium ionic liquid-functionalized SiO_2@graphene oxide as an additive, *ACS Appl. Mater. Interfaces* 13(42), 50573 (2021)
88. R. Tian, X. Jia, M. Lan, S. Wang, Y. Li, J. Yang, D. Shao, L. Feng, Q. Su, and H. Song, Ionic liquid crystals confining ultrathin MoS_2 nanosheets: A high-concen-

tration and stable aqueous dispersion, *ACS Sustain. Chem. & Eng.* 10(13), 4186 (2022)
89. N. G. Shang, P. Papakonstantinou, S. Sharma, G. Lubarsky, M. X. Li, D. W. McNeill, A. J. Quinn, W. Z. Zhou, and R. Blackley, Controllable selective exfoliation of high-quality graphene nanosheets and nanodots by ionic liquid assisted grinding, *Chem. Commun. (Camb.)* 48(13), 1877 (2012)
90. W. T. Zhang, Y. R. Wang, D. H. Zhang, S. X. Yu, W. X. Zhu, J. Wang, F. Q. Zheng, S. X. Wang, and J. L. Wang, A one-step approach to the large-scale synthesis of functionalized MoS_2 nanosheets by ionic liquid assisted grinding, *Nanoscale* 7(22), 10210 (2015)
91. S. Z. Bisri, S. Shimizu, M. Nakano, and Y. Iwasa, Endeavor of iontronics: From fundamentals to applications of ion-controlled electronics, *Adv. Mater.* 29(25), 1607054 (2017)
92. H. Yuan, H. Shimotani, A. Tsukazaki, A. Ohtomo, M. Kawasaki, and Y. Iwasa, High-density carrier accumulation in ZnO field-effect transistors gated by electric double layers of ionic liquids, *Adv. Funct. Mater.* 19(7), 1046 (2009)
93. S. Ono, N. Minder, Z. Chen, A. Facchetti, and A. F. Morpurgo, High-performance n-type organic field-effect transistors with ionic liquid gates, *Appl. Phys. Lett.* 97(14), 143307 (2010)
94. K. Hong, S. H. Kim, K. H. Lee, and C. D. Frisbie, Printed, sub-2V ZnO electrolyte gated transistors and inverters on plastic, *Adv. Mater.* 25(25), 3413 (2013)
95. K. Ueno, S. Nakamura, H. Shimotani, A. Ohtomo, N. Kimura, T. Nojima, H. Aoki, Y. Iwasa, and M. Kawasaki, Electric-field-induced superconductivity in an insulator, *Nat. Mater.* 7(11), 855 (2008)
96. J. T. Ye, S. Inoue, K. Kobayashi, Y. Kasahara, H. T. Yuan, H. Shimotani, and Y. Iwasa, Liquid-gated interface superconductivity on an atomically flat film, *Nat. Mater.* 9(2), 125 (2010)
97. K. Ueno, S. Nakamura, H. Shimotani, H. T. Yuan, N. Kimura, T. Nojima, H. Aoki, Y. Iwasa, and M. Kawasaki, Discovery of superconductivity in $KTaO_3$ by electrostatic carrier doping, *Nat. Nanotechnol.* 6(7), 408 (2011)
98. J. Ye, M. F. Craciun, M. Koshino, S. Russo, S. Inoue, H. Yuan, H. Shimotani, A. F. Morpurgo, and Y. Iwasa, Accessing the transport properties of graphene and its multilayers at high carrier density, *Proc. Natl. Acad. Sci. USA* 108(32), 13002 (2011)
99. A. T. Bollinger, G. Dubuis, J. Yoon, D. Pavuna, J. Misewich, and I. Bozovic, Superconductor–insulator transition in $La_{2-x}Sr_xCuO_4$ at the pair quantum resistance, *Nature* 472(7344), 458 (2011)
100. Y. Saito, Y. Nakamura, M. S. Bahramy, Y. Kohama, J. Ye, Y. Kasahara, Y. Nakagawa, M. Onga, M. Tokunaga, T. Nojima, Y. Yanase, Y. Iwasa, Superconductivity protected by spin-valley locking in ion-gated MoS_2, *Nat. Phys.* 12, 144 (2016)
101. Y. Yu, F. Yang, X. F. Lu, Y. J. Yan, Y. H. Cho, L. Ma, X. Niu, S. Kim, Y. W. Son, D. Feng, S. Li, S. W. Cheong, X. H. Chen, and Y. Zhang, Gate-tunable phase transitions in thin flakes of 1T-TaS_2, *Nat. Nanotechnol.* 10(3), 270 (2015)
102. Y. Saito, T. Nojima, and Y. Iwasa, Gate-induced superconductivity in two-dimensional atomic crystals, *Supercond. Sci. Technol.* 29(9), 093001 (2016)
103. Y. C. Wu, D. F. Li, C. L. Wu, H. Y. Hwang, and Y. Cui, Electrostatic gating and intercalation in 2D materials, *Nat. Rev. Mater.* (2022)
104. L. Liu, J. Han, L. Xu, J. Zhou, C. Zhao, S. Ding, H. Shi, M. Xiao, L. Ding, Z. Ma, C. Jin, Z. Zhang, and L. M. Peng, Aligned, high-density semiconducting carbon nanotube arrays for high-performance electronics, *Science* 368 (2020) 850
105. I. G. Lezama, A. Ubaldini, M. Longobardi, E. Giannini, C. Renner, A. B. Kuzmenko, and A. F. Morpurgo, Surface transport and band gap structure of exfoliated 2H-$MoTe_2$ crystals, *2D Mater.* 1, 021002 (2014)
106. F. L. Wang, P. Stepanov, M. Gray, C. N. Lau, M. E. Itkis, and R. C. Haddon, Ionic liquid gating of suspended MoS_2 field effect transistor devices, *Nano Lett.* 15(8), 5284 (2015)
107. W. Shi, J. T. Ye, Y. J. Zhang, R. Suzuki, M. Yoshida, J. Miyazaki, N. Inoue, Y. Saito, and Y. Iwasa, Superconductivity series in transition metal dichalcogenides by ionic gating, *Sci. Rep.* 5(1), 12534 (2015)
108. S. Larentis, J. R. Tolsma, B. Fallahazad, D. C. Dillen, K. Kim, A. H. MacDonald, and E. Tutuc, Band offset and negative compressibility in graphene–MoS_2 heterostructures, *Nano Lett.* 14(4), 2039 (2014)
109. G. Dezi, N. Scopigno, S. Caprara, and M. Grilli, Negative electronic compressibility and nanoscale inhomogeneity in ionic-liquid gated two-dimensional superconductors, *Phys. Rev. B* 98(21), 214507 (2018)
110. M. M. Ugeda, A. J. Bradley, Y. Zhang, S. Onishi, Y. Chen, W. Ruan, C. Ojeda-Aristizabal, H. Ryu, M. T. Edmonds, H. Z. Tsai, A. Riss, S. K. Mo, D. Lee, A. Zettl, Z. Hussain, Z. X. Shen, and M. F. Crommie, Characterization of collective ground states in single-layer $NbSe_2$, *Nat. Phys.* 12(1), 92 (2016)
111. A. W. Tsen, B. Hunt, Y. D. Kim, Z. J. Yuan, S. Jia, R. J. Cava, J. Hone, P. Kim, C. R. Dean, and A. N. Pasupathy, Nature of the quantum metal in a two-dimensional crystalline superconductor, *Nat. Phys.* 12, 208 (2016)
112. X. Xi, L. Zhao, Z. Wang, H. Berger, L. Forro, J. Shan, and K. F. Mak, Strongly enhanced charge-density-wave order in monolayer $NbSe_2$, *Nat. Nanotechnol.* 10, 765 (2015)
113. X. Xi, H. Berger, L. Forro, J. Shan, and K. F. Mak, Gate tuning of electronic phase transitions in two-dimensional $NbSe_2$, *Phys. Rev. Lett.* 117(10), 106801 (2016)
114. Y. Chen, W. Xing, X. Wang, B. Shen, W. Yuan, T. Su, Y. Ma, Y. Yao, J. Zhong, Y. Yun, X. C. Xie, S. Jia, and W. Han, Role of oxygen in ionic liquid gating on two-dimensional $Cr_2Ge_2Te_6$: A non-oxide material, *ACS Appl. Mater. Interfaces* 10(1), 1383 (2018)
115. C. Y. Cheng, W. L. Pai, Y. H. Chen, N. T. Paylaga, P. Y. Wu, C. W. Chen, C. T. Liang, F. C. Chou, R. Sankar, M. S. Fuhrer, S. Y. Chen, and W. H. Wang, Phase modulation of self-gating in ionic liquid-functionalized InSe field-effect transistors, *Nano Lett.* 22(6), 2270 (2022)

116. T. Xu, H. Du, H. Liu, W. Liu, X. Zhang, C. Si, P. Liu, and K. Zhang, Advanced nanocellulose-based composites for flexible functional energy storage devices, *Adv. Mater.* 33(48), 2101368 (2021)
117. S. Alipoori, S. Mazinani, S. H. Aboutalebi, and F. Sharif, Review of PVA-based gel polymer electrolytes in flexible solid-state supercapacitors: Opportunities and challenges, *J. Energy Storage* 27, 101072 (2020)
118. D. R. MacFarlane, N. Tachikawa, M. Forsyth, J. M. Pringle, P. C. Howlett, G. D. Elliott, J. H. Davis, M. Watanabe, P. Simon, and C. A. Angell, Energy applications of ionic liquids, *Energy Environ. Sci.* 7(1), 232 (2014)
119. Y. W. Chi, C. C. Hu, H. H. Shen, and K. P. Huang, New approach for high-voltage electrical double-layer capacitors using vertical graphene nanowalls with and without nitrogen doping, *Nano Lett.* 16(9), 5719 (2016)
120. A. Balducci, F. Soavi, and M. Mastragostino, The use of ionic liquids as solvent-free green electrolytes for hybrid supercapacitors, *Appl. Phys. A* 82, 627 (2006)
121. A. Balducci, W. A. Henderson, M. Mastragostino, S. Passerini, P. Simon, and F. Soavi, Cycling stability of a hybrid activated carbon//poly(3-methylthiophene) supercapacitor with N-butyl-N-methylpyrrolidinium bis(trifluoromethanesulfonyl)imide ionic liquid as electrolyte, *Electrochim. Acta* 50(11), 2233 (2005)
122. A. Balducci, U. Bardi, S. Caporali, M. Mastragostino, and F. Soavi, Ionic liquids for hybrid supercapacitors, *Electrochem. Commun.* 6(6), 566 (2004)
123. M. Mastragostino and F. Soavi, Strategies for high-performance supercapacitors for HEV, *J. Power Sources* 174(1), 89 (2007)
124. M. Galiński, A. Lewandowski, and I. Stepniak, Ionic liquids as electrolytes, *Electrochim. Acta* 51(26), 5567 (2006)
125. A. Lewandowski and M. Galinski, Carbon-ionic liquid double-layer capacitors, *J. Phys. Chem. Solids* 65(2–3), 281 (2004)
126. A. Balducci, R. Dugas, P. L. Taberna, P. Simon, D. Plee, M. Mastragostino, and S. Passerini, High temperature carbon-carbon supercapacitor using ionic liquid as electrolyte, *J. Power Sources* 165(2), 922 (2007)
127. C. Arbizzani, S. Beninati, M. Lazzari, F. Soavi, and M. Mastragostino, Electrode materials for ionic liquid-based supercapacitors, *J. Power Sources* 174(2), 648 (2007)
128. A. Eftekhari, Supercapacitors utilising ionic liquids, *Energy Storage Mater.* 9, 47 (2017)
129. R. Y. Lin, P. L. Taberna, S. Fantini, V. Presser, C. R. Perez, F. Malbosc, N. L. Rupesinghe, K. B. K. Teo, Y. Gogotsi, and P. Simon, Capacitive energy storage from –50 to 100 °C using an ionic liquid electrolyte, *J. Phys. Chem. Lett.* 2(19), 2396 (2011)
130. M. Kunze, S. Jeong, G. B. Appetecchi, M. Schöenhoff, M. Winter, and S. Passerini, Mixtures of ionic liquids for low temperature electrolytes, *Electrochim. Acta* 82, 69 (2012)
131. W. Y. Tsai, R. Lin, S. Murali, L. L. Zhang, J. K. McDonough, R. S. Ruoff, P. L. Taberna, Y. Gogotsi, and P. Simon, Outstanding performance of activated graphene based supercapacitors in ionic liquid electrolyte from –50 to 80 °C, *Nano Energy* 2(3), 403 (2013)
132. C. Lethien, J. Le Bideau, and T. Brousse, Challenges and prospects of 3D micro-supercapacitors for powering the internet of things, *Energy Environ. Sci.* 12(1), 96 (2019)
133. Z. Yang, J. Tian, Z. Yin, C. Cui, W. Qian, and F. Wei, Carbon nanotube- and graphene-based nanomaterials and applications in high-voltage supercapacitor: A review, *Carbon* 141, 467 (2019)
134. C. Cui, W. Qian, Y. Yu, C. Kong, B. Yu, L. Xiang, and F. Wei, Highly electroconductive mesoporous graphene nanofibers and their capacitance performance at 4 V, *J. Am. Chem. Soc.* 136(6), 2256 (2014)
135. Y. Yu, C. Cui, W. Qian, and F. Wei, Full capacitance potential of SWCNT electrode in ionic liquids at 4 V, *J. Mater. Chem. A* 2(46), 19897 (2014)
136. M. Lazzari, M. Mastragostino, and F. Soavi, Capacitance response of carbons in solvent-free ionic liquid electrolytes, *Electrochem. Commun.* 9(7), 1567 (2007)
137. D. R. MacFarlane, P. Meakin, J. Sun, N. Amini, and M. Forsyth, Pyrrolidinium imides: A new family of molten salts and conductive plastic crystal phases, *J. Phys. Chem. B* 103(20), 4164 (1999)
138. W. A. Henderson and S. Passerini, Phase behavior of ionic liquid-LiX mixtures: Pyrrolidinium cations and TFSI- anions, *Chem. Mater.* 16(15), 2881 (2004)
139. Y. Zhou, H. Qi, J. Yang, Z. Bo, F. Huang, M. S. Islam, X. Lu, L. Dai, R. Amal, C. H. Wang, and Z. Han, Two-birds-one-stone: Multifunctional supercapacitors beyond traditional energy storage, *Energy Environ. Sci.* 14(4), 1854 (2021)
140. G. Lota, K. Fic, and E. Frackowiak, Carbon nanotubes and their composites in electrochemical applications, *Energy Environ. Sci.* 4(5), 1592 (2011)
141. M. F. El-Kady, Y. L. Shao, and R. B. Kaner, Graphene for batteries, supercapacitors and beyond, *Nat. Rev. Mater.* 1(7), 16033 (2016)
142. A. G. Pandolfo and A. F. Hollenkamp, Carbon properties and their role in supercapacitors, *J. Power Sources* 157(1), 11 (2006)
143. L. Hao, J. Ning, B. Luo, B. Wang, Y. Zhang, Z. Tang, J. Yang, A. Thomas, and L. Zhi, Structural evolution of 2D microporous covalent triazine-based framework toward the study of high-performance supercapacitors, *J. Am. Chem. Soc.* 137(1), 219 (2015)
144. Y. W. Zhu, S. Murali, M. D. Stoller, K. J. Ganesh, W. W. Cai, P. J. Ferreira, A. Pirkle, R. M. Wallace, K. A. Cychosz, M. Thommes, D. Su, E. A. Stach, and R. S. Ruoff, Carbon-based supercapacitors produced by activation of graphene, *Science* 332(6037), 1537 (2011)
145. C. Largeot, C. Portet, J. Chmiola, P.-L. Taberna, Y. Gogotsi, P. Simon, Relation between the ion size and pore size for an electric double-layer capacitor, *J. Am. Chem. Soc.* 130, 2730 (2008)
146. J. Chmiola, G. Yushin, Y. Gogotsi, C. Portet, P. Simon, and P. L. Taberna, Anomalous increase in carbon capacitance at pore sizes less than 1 nanometer, *Science* 313(5794), 1760 (2006)
147. C. Zheng, W. Z. Qian, C. J. Cui, Q. Zhang, Y. G. Jin, M. Q. Zhao, P. H. Tan, and F. Wei, Hierarchical carbon nanotube membrane with high packing density

and tunable porous structure for high voltage supercapacitors, *Carbon* 50(14), 5167 (2012)
148. Y. S. Yun, S. Y. Cho, J. Shim, B. H. Kim, S. J. Chang, S. J. Baek, Y. S. Huh, Y. Tak, Y. W. Park, S. Park, and H. J. Jin, Microporous carbon nanoplates from regenerated silk proteins for supercapacitors, *Adv. Mater.* 25(14), 1993 (2013)
149. Z. B. Lei, Z. H. Liu, H. J. Wang, X. X. Sun, L. Lu, and X. S. Zhao, A high-energy-density supercapacitor with graphene-CMK-5 as the electrode and ionic liquid as the electrolyte, *J. Mater. Chem. A* 1(6), 2313 (2013)
150. T. Kim, H. C. Kang, T. Tran Thanh, J. D. Lee, H. Kim, W. S. Yang, H. G. Yoon, and K. S. Suh, Ionic liquid-assisted microwave reduction of graphite oxide for supercapacitors, *RSC Adv.* 2(23), 8808 (2012)
151. H. Wang, Z. Xu, A. Kohandehghan, Z. Li, K. Cui, X. Tan, T. J. Stephenson, C. K. King'ondu, C. M. B. Holt, B. C. Olsen, J. K. Tak, D. Harfield, A. O. Anyia, and D. Mitlin, Interconnected carbon nanosheets derived from hemp for ultrafast supercapacitors with high energy, *ACS Nano* 7(6), 5131 (2013)
152. L. L. Zhang, X. Zhao, M. D. Stoller, Y. Zhu, H. Ji, S. Murali, Y. Wu, S. Perales, B. Clevenger, and R. S. Ruoff, Highly conductive and porous activated reduced graphene oxide films for high-power supercapacitors, *Nano Lett.* 12(4), 1806 (2012)
153. N. Jung, S. Kwon, D. Lee, D. M. Yoon, Y. M. Park, A. Benayad, J. Y. Choi, and J. S. Park, Synthesis of chemically bonded graphene/carbon nanotube composites and their application in large volumetric capacitance supercapacitors, *Adv. Mater.* 25(47), 6854 (2013)
154. G. P. Hao, A. H. Lu, W. Dong, Z. Y. Jin, X. Q. Zhang, J. T. Zhang, and W. C. Li, Sandwich-type microporous carbon nanosheets for enhanced supercapacitor performance, *Adv. Energy Mater.* 3(11), 1421 (2013)
155. T. Brousse, D. Belanger, and J. W. Long, To be or not to be pseudocapacitive, *J. Electrochem. Soc.* 162(5), A5185 (2015)
156. P. Simon, Y. Gogotsi, and B. Dunn, Where do batteries end and supercapacitors begin, *Science* 343(6176), 1210 (2014)
157. B. E. Conway, Transition from supercapacitor to battery behavior in electrochemical energy-storage, *J. Electrochem. Soc.* 138(6), 1539 (1991)
158. E. Mourad, L. Coustan, P. Lannelongue, D. Zigah, A. Mehdi, A. Vioux, S. A. Freunberger, F. Favier, O. Fontaine, Biredox ionic liquids with solid-like redox density in the liquid state for high-energy supercapacitors, *Nat. Mater.* 16, 446 (2017)
159. P. Simon and Y. Gogotsi, Perspectives for electrochemical capacitors and related devices, *Nat. Mater.* 19(11), 1151 (2020)
160. Y. Jing, Z. Zhou, C. R. Cabrera, and Z. Chen, Graphene, inorganic graphene analogs and their composites for lithium ion batteries, *J. Mater. Chem. A* 2(31), 12104 (2014)
161. M. K. Aslam, Y. B. Niu, and M. W. Xu, MXenes for non-lithium-ion (Na, K, Ca, Mg, and Al) batteries and supercapacitors, *Adv. Energy Mater.* 11(2), 2000681 (2021)
162. A. Peigney, C. Laurent, E. Flahaut, R. R. Bacsa, and A. Rousset, Specific surface area of carbon nanotubes and bundles of carbon nanotubes, *Carbon* 39(4), 507 (2001)
163. J. Wang, B. Ding, Y. Xu, L. Shen, H. Dou, and X. Zhang, Crumpled nitrogen-doped graphene for supercapacitors with high gravimetric and volumetric performances, *ACS Appl. Mater. Interfaces* 7(40), 22284 (2015)
164. X. Yang, C. Cheng, Y. Wang, L. Qiu, and D. Li, Liquid-mediated dense integration of graphene materials for compact capacitive energy storage, *Science* 341(6145), 534 (2013)
165. R. Futamura, T. Iiyama, Y. Takasaki, Y. Gogotsi, M. J. Biggs, M. Salanne, J. Segalini, P. Simon, K. Kaneko, Partial breaking of the Coulombic ordering of ionic liquids confined in carbon nanopores, *Nat. Mater.* 16, 1225 (2017)
166. Z. N. Li, S. Gadipelli, H. C. Li, C. A. Howard, D. J. L. Brett, P. R. Shearing, Z. X. Guo, I. P. Parkin, and F. Li, Tuning the interlayer spacing of graphene laminate films for efficient pore utilization towards compact capacitive energy storage, *Nat. Energy* 5(2), 160 (2020)
167. C. Cheng, G. Jiang, G. P. Simon, J. Z. Liu, and D. Li, Low-voltage electrostatic modulation of ion diffusion through layered graphene-based nanoporous membranes, *Nat. Nanotechnol.* 13, 685 (2018)
168. X. L. Su, C. R. Ye, X. P. Li, M. H. Guo, R. G. Cao, K. Ni, and Y. W. Zhu, Heterogeneous stacking carbon films for optimized supercapacitor performance, *Energy Storage Mater.* 50, 365 (2022)
169. J. Kim and S. Kim, Preparation and electrochemical property of ionic liquid-attached graphene nanosheets for an application of supercapacitor electrode, *Electrochim. Acta* 119, 11 (2014)
170. J. Kim and S. Kim, Surface-modified reduced graphene oxide electrodes for capacitors by ionic liquids and their electrochemical properties, *Appl. Surf. Sci.* 295, 31 (2014)
171. B. Anasori, Y. Xie, M. Beidaghi, J. Lu, B. C. Hosler, L. Hultman, P. R. C. Kent, Y. Gogotsi, and M. W. Barsoum, Two-dimensional, ordered, double transition metals carbides (MXenes), *ACS Nano* 9(10), 9507 (2015)
172. Q. Hu, D. Sun, Q. Wu, H. Wang, L. Wang, B. Liu, A. Zhou, and J. He, MXene: A new family of promising hydrogen storage medium, *J. Phys. Chem. A* 117(51), 14253 (2013)
173. Y. Dong, S. Zheng, J. Qin, X. Zhao, H. Shi, X. Wang, J. Chen, and Z. S. Wu, All-MXene-based integrated electrode constructed by Ti_3C_2 nanoribbon framework host and nanosheet interlayer for high-energy-density Li-S batteries, *ACS Nano* 12(3), 2381 (2018)
174. M. R. Lukatskaya, O. Mashtalir, C. E. Ren, Y. Dall' Agnese, P. Rozier, P. L. Taberna, M. Naguib, P. Simon, M. W. Barsoum, and Y. Gogotsi, Cation intercalation and high volumetric capacitance of two-dimensional titanium carbide, *Science* 341(6153), 1502 (2013)
175. A. VahidMohammadi, J. Moncada, H. Chen, E. Kayali, J. Orangi, C. A. Carrero, and M. Beidaghi, Thick and freestanding MXene/PANI pseudocapacitive electrodes

with ultrahigh specific capacitance, *J. Mater. Chem. A* 6(44), 22123 (2018)
176. M. Lu, H. J. Li, W. J. Han, J. N. Chen, W. Shi, J. H. Wang, X. M. Meng, J. G. Qi, H. B. Li, B. S. Zhang, W. Zhang, and W. Zheng, 2D titanium carbide (MXene) electrodes with lower-F surface for high performance lithium-ion batteries, *J. Energy Chem.* 31, 148 (2019)
177. F. Wu, Y. Jiang, Z. Q. Ye, Y. X. Huang, Z. H. Wang, S. J. Li, Y. Mei, M. Xie, L. Li, and R. J. Chen, A 3D flower-like VO_2/MXene hybrid architecture with superior anode performance for sodium ion batteries, *J. Mater. Chem. A* 7(3), 1315 (2019)
178. Y. Xia, T. S. Mathis, M. Q. Zhao, B. Anasori, A. Dang, Z. H. Zhou, H. Cho, Y. Gogotsi, and S. Yang, Thickness - independent capacitance of vertically aligned liquid-crystalline MXenes, *Nature* 557, 409 (2018)
179. C. F. Zhang, M. P. Kremer, A. Seral-Ascaso, S. H. Park, N. McEvoy, B. Anasori, Y. Gogotsi, and V. Nicolosi, Stamping of flexible, coplanar micro-supercapacitors using MXene inks, *Adv. Funct. Mater.* 28(9), 1705506 (2018)
180. S. Xu, Y. Dall'Agnese, G. Wei, C. Zhang, Y. Gogotsi, and W. Han, Screen-printable microscale hybrid device based on MXene and layered double hydroxide electrodes for powering force sensors, *Nano Energy* 50, 479 (2018)
181. Z. Lin, D. Barbara, P. L. Taberna, K. L. Van Aken, B. Anasori, Y. Gogotsi, and P. Simon, Capacitance of $Ti_3C_2T_x$ MXene in ionic liquid electrolyte, *J. Power Sources* 326, 575 (2016)
182. Z. F. Lin, P. Rozier, B. Duployer, P. L. Taberna, B. Anasori, Y. Gogotsi, and P. Simon, Electrochemical and in-situ X-ray diffraction studies of $Ti_3C_2T_x$ MXene in ionic liquid electrolyte, *Electrochem. Commun.* 72, 50 (2016)
183. S. H. Zheng, C. Zhang, F. Zhou, Y. F. Dong, X. Y. Shi, V. Nicolosi, Z. S. Wu, and X. H. Bao, Ionic liquid pre-intercalated MXene films for ionogel-based flexible micro-supercapacitors with high volumetric energy density, *J. Mater. Chem. A* 7(16), 9478 (2019)
184. O. D. Bakulina, M. Y. Ivanov, S. A. Prikhod'ko, S. Pylaeva, I. V. Zaytseva, N. V. Surovtsev, N. Y. Adonin, and M. V. Fedin, Nanocage formation and structural anomalies in imidazolium ionic liquid glasses governed by alkyl chains of cations, *Nanoscale* 12(38), 19982 (2020)
185. K. Liang, R. A. Matsumoto, W. Zhao, N. C. Osti, I. Popov, B. P. Thapaliya, S. Fleischmann, S. Misra, K. Prenger, M. Tyagi, E. Mamontov, V. Augustyn, R. R. Unocic, A. P. Sokolov, S. Dai, P. T. Cummings, and M. Naguib, Engineering the interlayer spacing by pre-intercalation for high performance supercapacitor MXene electrodes in room temperature ionic liquid, *Adv. Funct. Mater.* 31(33), 2104007 (2021)
186. Q. Fan, R. Z. Zhao, M. J. Yi, P. Qi, C. X. Chai, H. Ying, and J. C. Hao, Ti_3C_2-MXene composite films functionalized with polypyrrole and ionic liquid-based microemulsion particles for supercapacitor applications, *Chem. Eng. J.* 428, 131107 (2022)
187. Y. J. Wan, K. Rajavel, X. M. Li, X. Y. Wang, S. Y. Liao, Z. Q. Lin, P. L. Zhu, R. Sun, and C. P. Wong, Electromagnetic interference shielding of $Ti_3C_2T_x$ MXene modified by ionic liquid for high chemical stability and excellent mechanical strength, *Chem. Eng. J.* 408, 127303 (2021)
188. J. S. Lee, X. Q. Wang, H. M. Luo, G. A. Baker, and S. Dai, Facile ionothermal synthesis of microporous and mesoporous carbons from task specific ionic liquids, *J. Am. Chem. Soc.* 131, 4596 (2009)
189. Y. Yoshida, K. Fujie, D. W. Lim, R. Ikeda, and H. Kitagawa, Superionic conduction over a wide temperature range in a metal-organic framework impregnated with ionic liquids, *Angew. Chem. Int. Ed.* 58(32), 10909 (2019)
190. S. Bi, H. Banda, M. Chen, L. Niu, M. Chen, T. Wu, J. Wang, R. Wang, J. Feng, T. Chen, M. Dinca, A. A. Kornyshev, and G. Feng, Molecular understanding of charge storage and charging dynamics in supercapacitors with MOF electrodes and ionic liquid electrolytes, *Nat. Mater.* 19, 552 (2020)
191. C. Zhong, Y. Deng, W. Hu, J. Qiao, L. Zhang, and J. Zhang, A review of electrolyte materials and compositions for electrochemical supercapacitors, *Chem. Soc. Rev.* 44(21), 7484 (2015)
192. H. Yang, S. Kannappan, A. S. Pandian, J. H. Jang, Y. S. Lee, and W. Lu, Graphene supercapacitor with both high power and energy density, *Nanotechnology* 28(44), 445401 (2017)
193. A. González, E. Goikolea, J. Andoni Barrena, and R. Mysyk, Review on supercapacitors: Technologies and materials, *Renew. Sustain. Energy Rev.* 58, 1189 (2016)
194. S. Pohlmann, R. S. Kühnel, T. A. Centeno, and A. Balducci, The influence of anion-cation combinations on the physicochemical properties of advanced electrolytes for supercapacitors and the capacitance of activated carbons, *ChemElectroChem* 1(8), 1301 (2014)
195. K. L. Van Aken, M. Beidaghi, and Y. Gogotsi, Formulation of ionic-liquid electrolyte to expand the voltage window of supercapacitors, *Angew. Chem. Int. Ed.* 54(16), 4806 (2015)
196. S. Pohlmann, C. Ramirez-Castro, and A. Balducci, The influence of conductive salt ion selection on EDLC electrolyte characteristics and carbon-electrolyte interaction, *J. Electrochem. Soc.* 162(5), A5020 (2015)
197. W. Q. Ye, H. Y. Wang, J. Q. Ning, Y. J. Zhong, and Y. Hu, New types of hybrid electrolytes for supercapacitors, *J. Energy Chem.* 57, 219 (2021)
198. R. Hagiwara, K. Matsumoto, Y. Nakamori, T. Tsuda, Y. Ito, H. Matsumoto, and K. Momota, Physicochemical properties of 1, 3-dialkylimidazolium fluorohydrogenate room-temperature molten salts, *J. Electrochem. Soc.* 150(12), D195 (2003)
199. C. Kong, W. Qian, C. Zheng, Y. Yu, C. Cui, and F. Wei, Raising the performance of a 4 V supercapacitor based on an EMIBF4-single walled carbon nanotube nanofluid electrolyte, *Chem. Commun. (Camb.)* 49(91), 10727 (2013)
200. D. Yang, X. Zhou, R. X. Yang, Z. Yang, W. Yu, X. L. Wang, C. Li, S. Z. Liu, and R. P. H. Chang, Surface optimization to eliminate hysteresis for record efficiency planar perovskite solar cells, *Energy Environ. Sci.*

9(10), 3071 (2016)
201. S. Bai, P. M. Da, C. Li, Z. P. Wang, Z. C. Yuan, F. Fu, M. Kawecki, X. J. Liu, N. Sakai, J. T. W. Wang, S. Huettner, S. Buecheler, M. Fahlman, F. Gao, and H. J. Snaith, Planar perovskite solar cells with long-term stability using ionic liquid additives, *Nature* 571, 245 (2019)
202. G. Divitini, S. Cacovich, F. Matteocci, L. Cina, A. Di Carlo, and C. Ducati, *In situ* observation of heat-induced degradation of perovskite solar cells, *Nat. Energy* 1(2), 15012 (2016)
203. T. Leijtens, E. T. Hoke, G. Grancini, D. J. Slotcavage, G. E. Eperon, J. M. Ball, M. De Bastiani, A. R. Bowring, N. Martino, K. Wojciechowski, M. D. McGehee, H. J. Snaith, and A. Petrozza, Mapping electric field-induced switchable poling and structural degradation in hybrid lead halide perovskite thin films, *Adv. Energy Mater.* 5(20), 1500962 (2015)
204. K. Domanski, B. Roose, T. Matsui, M. Saliba, S. H. Turren-Cruz, J. P. Correa-Baena, C. Roldan-Carmona, G. Richardson, J. M. Foster, F. De Angelis, J. M. Ball, A. Petrozza, N. Mine, M. K. Nazeeruddin, W. Tress, M. Grätzel, U. Steiner, A. Hagfeldt, and A. Abate, Migration of cations induces reversible performance losses over day/night cycling in perovskite solar cells, *Energy Environ. Sci.* 10(2), 604 (2017)
205. X. J. Zhu, M. Y. Du, J. S. Feng, H. Wang, Z. Xu, L. K. Wang, S. N. Zuo, C. Y. Wang, Z. Y. Wang, C. Zhang, X. D. Ren, S. Priya, D. Yang, and S. Liu, High-efficiency perovskite solar cells with imidazolium-based ionic liquid for surface passivation and charge transport, *Angew. Chem. Int. Ed.* 60(8), 4238 (2021)
206. X. Wang, X. Ran, X. Liu, H. Gu, S. Zuo, W. Hui, H. Lu, B. Sun, X. Gao, J. Zhang, Y. Xia, Y. Chen, and W. Huang, Tailoring component interaction for air-processed efficient and stable all-inorganic perovskite photovoltaic, *Angew. Chem. Int. Ed.* 59(32), 13354 (2020)
207. C. Liu, Z. Fang, J. S. Sun, Q. Lou, J. F. Ge, X. Chen, E. J. Zhou, M. H. Shang, W. Y. Yang, and Z. Y. Ge, Imidazolium ionic liquid as organic spacer for tuning the excitonic structure of 2D perovskite materials, *ACS Energy Lett.* 5(11), 3617 (2020)
208. W. Hui, L. F. Chao, H. Lu, F. Xia, Q. Wei, et al., Stabilizing black-phase formamidinium perovskite formation at room temperature and high humidity, *Science* 371, 1359 (2021)
209. A. K. Geim and I. V. Grigorieva, Van der Waals heterostructures, *Nature* 499(7459), 419 (2013)
210. Y. F. Sun, S. Gao, and Y. Xie, Atomically-thick two-dimensional crystals: Electronic structure regulation and energy device construction, *Chem. Soc. Rev.* 43(2), 530 (2014)
211. X. Huang, C. Tan, Z. Yin, and H. Zhang, 25th anniversary article: Hybrid nanostructures based on two-Dimensional nanomaterials, *Adv. Mater.* 26(14), 2185 (2014)
212. Y. Sun, S. Gao, F. Lei, C. Xiao, and Y. Xie, Ultrathin two-dimensional inorganic materials: New opportunities for solid state nanochemistry, *Acc. Chem. Res.* 48(1), 3 (2015)
213. Y. Sun, H. Cheng, S. Gao, Z. Sun, Q. Liu, Q. Liu, F. Lei, T. Yao, J. He, S. Wei, and Y. Xie, Freestanding tin disulfide single-layers realizing efficient visible-light water splitting, *Angew. Chem. Int. Ed.* 51(35), 8727 (2012)
214. J. Li, Y. Yu, and L. Zhang, Bismuth oxyhalide nanomaterials: Layered structures meet photocatalysis, *Nanoscale* 6(15), 8473 (2014)
215. J. Jiang, K. Zhao, X. Xiao, and L. Zhang, Synthesis and facet-dependent photoreactivity of BiOCl Single-crystalline nanosheets, *J. Am. Chem. Soc.* 134(10), 4473 (2012)
216. J. Łuczak, M. Paszkiewicz, A. Krukowska, A. Malankowska, and A. Zaleska-Medynska, Ionic liquids for nano- and microstructures preparation (Part 1): Properties and multifunctional role, *Adv. Colloid Interface Sci.* 230, 13 (2016)
217. J. Łuczak, M. Paszkiewicz, A. Krukowska, A. Malankowska, and A. Zaleska-Medynska, Ionic liquids for nano- and microstructures preparation (Part 2): Application in synthesis, *Adv. Colloid Interface Sci.* 227, 1 (2016)
218. L. Dou, Y. Xiang, J. Zhong, J. Li, and S. Huang, Ionic liquid-assisted preparation of thin Bi_2SiO_5 nanosheets for effective photocatalytic degradation of RhB, *Mater. Lett.* 261, 127117 (2020)
219. J. Xia, M. Ji, J. Di, B. Wang, S. Yin, M. He, Q. Zhang, and H. Li, Improved photocatalytic activity of few-layer $Bi_4O_5I_2$ nanosheets induced by efficient charge separation and lower valence position, *J. Alloys Compd.* 695, 922 (2017)
220. J. H. Li, J. Ren, Y. J. Hao, E. P. Zhou, Y. Wang, X. J. Wang, R. Su, Y. Liu, X. H. Qi, and F. T. Li, Construction of beta-Bi_2O_3/$Bi_2O_2CO_3$ heterojunction photocatalyst for deep understanding the importance of separation efficiency and valence band position, *J. Hazard. Mater.* 401, 123262 (2021)
221. M. K. Jana, K. Biswas, and C. N. R. Rao, Ionothermal synthesis of few-layer nanostructures of Bi_2Se_3 and related materials, *Chemistry* 19(28), 9110 (2013)
222. J. Z. Zhao, M. X. Ji, J. Di, Y. P. Ge, P. F. Zhang, J. X. Xia, and H. M. Li, Synthesis of g-C_3N_4/$Bi_4O_5Br_2$ via reactable ionic liquid and its cooperation effect for the enhanced photocatalytic behavior towards ciprofloxacin degradation, *J. Photochem. Photobiol. A* 347, 168 (2017)
223. Q. Y. Zhu, Z. Y. Wang, L. F. Chen, H. Y. Cheng, and Z. W. Qi, Ionic-liquid-controlled two-dimensional monolayer Bi_2MoO_6 and its adsorption of azo molecules, *ACS Appl. Nano Mater.* 1(9), 5083 (2018)
224. A. Pancielejko, J. Luczak, W. Lisowski, G. Trykowski, D. Venieri, A. Zaleska-Medynska, and P. Mazierski, Ionic liquid as morphology-directing agent of two-dimensional Bi_2WO_6: New insight into photocatalytic and antibacterial activity, *Appl. Surf. Sci.* 599, 153971 (2022)
225. M. Peplow, Graphene booms in factories but lacks a killer app, *Nature* 522(7556), 268 (2015)
226. S. Ravula, S. N. Baker, G. Kamath, and G. A. Baker, Ionic liquid-assisted exfoliation and dispersion: stripping graphene and its two-dimensional layered inorganic

counterparts of their inhibitions, *Nanoscale* 7(10), 4338 (2015)

227. J. Lu, J. Yang, J. Wang, A. Lim, S. Wang, and K. P. Loh, One-pot synthesis of fluorescent carbon nanoribbons, nanoparticles, and graphene by the exfoliation of graphite in ionic liquids, *ACS Nano* 3(8), 2367 (2009)
228. Y. Zhang, S. W. Li, Y. X. Xu, X. Y. Shi, M. X. Zhang, Y. N. Huang, Y. Liang, Y. Q. Chen, W. L. Ji, J. R. Kim, W. L. Song, D. G. Yu, and I. Kim, Engineering of hollow polymeric nanosphere-supported imidazolium-based ionic liquids with enhanced antimicrobial activities, *Nano Res.* 15(6), 5556 (2022)
229. S. Tajik, A. Lohrasbi-Nejad, P. Mohammadzadeh Jahani, M. B. Askari, P. Salarizadeh, and H. Beitollahi, Co-detection of carmoisine and tartrazine by carbon paste electrode modified with ionic liquid and MoO_3/WO_3 nanocomposite, *J. Food Meas. Charact.* 16(1), 722 (2022)
230. F. G. Nejad, I. Sheikhshoaie, and H. Beitollahi, Simultaneous detection of carmoisine and tartrazine in food samples using GO-Fe_3O_4-PAMAM and ionic liquid based electrochemical sensor, *Food Chem. Toxicol.* 162, 112864 (2022)
231. H. Karimi-Maleh, R. Darabi, M. Shabani-Nooshabadi, M. Baghayeri, F. Karimi, J. Rouhi, M. Alizadeh, O. Karaman, Y. Vasseghian, and C. Karaman, Determination of D&C Red 33 and Patent Blue V Azo dyes using an impressive electrochemical sensor based on carbon paste electrode modified with ZIF-8/g-C_3N_4/Co and ionic liquid in mouthwash and toothpaste as real samples, *Food Chem. Toxicol.* 162, 112907 (2022)
232. M. Degani, Q. Z. An, M. Albaladejo-Siguan, Y. J. Hofstetter, C. Cho, F. Paulus, G. Grancini, and Y. Vaynzof, 23.7% efficient inverted perovskite solar cells by dual interfacial modification, *Sci. Adv.* 7(49), eabj7930 (2021)
233. G. Zeng, W. J. Chen, X. B. Chen, Y. Hu, Y. Chen, B. Zhang, H. Y. Chen, W. W. Sun, Y. X. Shen, Y. W. Li, F. Yan, and Y. F. Li, Realizing 17.5% efficiency flexible organic solar cells via atomic-level chemical welding of silver nanowire electrodes, *J. Am. Chem. Soc.* 144(19), 8658 (2022)